

2018

# Earlier onset of cognitive deficits and an upregulated neuroinflammatory response in the chronic phase after stroke in obese mice

---

<https://hdl.handle.net/2144/31240>

*"Downloaded from OpenBU. Boston University's institutional repository."*

BOSTON UNIVERSITY  
SCHOOL OF MEDICINE

Thesis

**EARLIER ONSET OF COGNITIVE DEFICITS AND AN UPREGULATED  
NEUROINFLAMMATORY RESPONSE IN THE CHRONIC PHASE AFTER  
STROKE IN OBESE MICE**

by

**AUSTIN LUI**

B.S., University of California, Davis, 2015

Submitted in partial fulfillment of the  
requirements for the degree of  
Master of Science

2018

© 2018 by  
AUSTIN LUI  
All rights reserved

Approved by

First Reader

---

C. James McKnight, Ph.D.  
Associate Professor of Physiology and Biophysics

Second Reader

---

S. Marion Buckwalter, M.D, Ph.D.  
Associate Professor of Neurology and Neurosurgery

## **ACKNOWLEDGMENTS**

I would like to thank Marion Buckwalter, Todd Peterson, James McKnight, and the entire Buckwalter Laboratory for all the guidance and help given to me for my project.

**EARLIER ONSET OF COGNITIVE DEFICITS AND AN UPREGULATED  
NEUROINFLAMMATORY RESPONSE IN THE CHRONIC PHASE AFTER  
STROKE IN OBESE MICE**

**AUSTIN LUI**

**ABSTRACT**

Stroke is a neurovascular disease that frequently results in decreased motor and cognitive functioning. Obesity is a major risk factor associated with ischemic stroke and is thought to worsen the functional deficits observed after stroke. Previous findings from our laboratory suggest that worse motor deficits in obese animals may be a result from an exacerbated neuroinflammatory response. Most animal studies demonstrate an association between obesity and worse cognitive functioning after stroke. However, the mechanisms are not well studied. This study examines the neuroinflammatory response, ischemic brain tissue damage, and cognitive functioning in diet-induced obese mouse models during the chronic phase after ischemic stroke, defined as weeks after stroke. Our study found an earlier onset of cognitive deficits in obese mice after stroke compared to normal weight mice. We found no differences in the degree of brain damage in obese animals and normal weight animals 11 weeks after stroke, but observed higher levels of microgliosis in obese animals compared to normal weight animals. Due to the limitations of our study, additional studies should be done to assess the severity of cognitive deficits in obese animals compared to normal weight animals in the chronic phase after stroke.

Further studies also need to be done to confirm our findings regarding the microglial response and degree of ischemic brain damage during the chronic phase.

## TABLE OF CONTENTS

TITLE	i
COPYRIGHT PAGE	ii
READER APPROVAL PAGE	iii
ACKNOWLEDGMENTS	iv
ABSTRACT	v
TABLE OF CONTENTS	vii
LIST OF FIGURES	viii
LIST OF ABBREVIATIONS	xi
INTRODUCTION	1
METHODS	31
RESULTS	40
DISCUSSION	61
REFERENCES	73
CURRICULUM VITAE	99

## LIST OF FIGURES

Figure	Title	Page
1	Experimental timeline: Diet feeding and behavior schedule relative to stroke.	32
2	Schematic of Y-maze paradigm.	37
3	Schematic of Novel Object Task paradigm.	39
4	The percent of original weight for normal diet-fed animals and HFD-fed animal at weeks 1, 2, 3, 4, 5, and 6 from another previous study.	41
5	The percent of original weight for normal diet-fed animals and HFD-fed animal at weeks 1, 2, 3, 4, 5, and 6 from another previous study.	42
6	The percent Y-Maze alternation in Sham-normal diet, Sham-HFD, dMCAO-normal diet, and dMCAO-HFD groups at baseline prior to surgery and at 1, 4, 7, 11 weeks after surgery.	43
7	The percent NO contacts in Sham-normal diet, Sham-HFD, dMCAO-normal diet, and dMCAO-HFD groups at baseline prior to surgery and at 1, 4, 7, 11 weeks after surgery.	45

8	The percent time near NO in Sham-normal diet, Sham-HFD, dMCAO-normal diet, and dMCAO-HFD groups at baseline prior to surgery and at 1, 4, 7, 11 weeks after surgery.	46
9	The infarct area as a percent of contralateral hemisphere area for dMCAO-normal diet and dMCAO-HFD group.	48
10	Ipsilateral hemisphere area as a percent of contralateral hemisphere area for the dMCAO-normal diet and dMCAO-HFD diet group.	49
11	Ipsilateral cortical area as a percent of the contralateral cortical area for dMCAO-normal diet and dMCAO-HFD group.	50
12	Relative percent area GFAP in Sham-normal diet, Sham-HFD, dMCAO-normal diet, and dMCAO-HFD groups using less inclusive thresholding.	51
13	Relative percent area GFAP in Sham-normal diet, Sham-HFD, dMCAO-normal diet, and dMCAO-HFD groups using more inclusive thresholding.	52
14	Relative percent area CD68 in Sham-normal diet, Sham-HFD, dMCAO-normal diet, and dMCAO-HFD groups using less inclusive thresholding.	54

15	Relative percent area CD68 in Sham-normal diet, Sham-HFD, dMCAO-normal diet, and dMCAO-HFD groups using more inclusive thresholding.	55
16	Multiple regression analysis between ipsilateral cortex area percent of contralateral cortex area and weight for dMCAO-normal diet and dMCAO-HFD group.	56
17	Percent alternation for Y-maze task at weeks 1, 4, 7, 11 after surgery vs weight at sacrifice for dMCAO-normal diet and dMCAO-HFD group.	57
18	Relative percent area GFAP with more inclusive thresholding vs weight for dMCAO-normal diet and dMCAO-HFD group.	58
19	Relative percent area CD68 with more inclusive thresholding vs weight for dMCAO-normal diet and dMCAO-HFD group.	60

## LIST OF ABBREVIATIONS

ANOVA	analysis of variance
APC	antigen-presenting cell
ATP	adenosine triphosphate
BBB	blood brain barrier
BMI	body mass index
Bregs	regulatory B-cells
CINC	cytokine-induced neutrophil chemoattractant
CCL-3	C-C motif ligand-3
CCR-2	C-C chemokine receptor type 2
CNS	central nervous system
CXCL	C-X-C motif ligand
DAMP	damage-associated molecular pattern
Db/db	leptin-receptor deficiency
DH	distal hypoxic
dMCAO	distal middle cerebral artery occlusion
ECM	extracellular matrix
FasL	first apoptosis signal receptor ligand
FFA	free fatty acid
GFAP	glial fibrillary acid protein

GLUT-4	glucose transporter type-4
HFD	high-fat diet
ICAM-1	intercellular adhesion molecule-1
IFN - $\gamma$	interferon gamma
IgA	immunoglobulin-A
IgG	immunoglobulin-G
IgG1	immunoglobulin-G 1
IgG2	immunoglobulin-G 2
IL-1	interleukin-1
IL-1 $\beta$	interleukin-1 beta
IL-4	interleukin-4
IL-5	interleukin-5
IL-6	interleukin-6
IL-10	interleukin-10
IL-13	interleukin-13
IL-18	interleukin-18
IL-22	interleukin-22
IL-35	interleukin-35
iNOS	inducible nitric oxide synthase
IRF	interferon regulatory factor
Ob/ob	leptin-deficiency
LTP	long-term potentiation

MCA	middle cerebral artery
MCAO	middle cerebral artery occlusion
MCP-1	monocyte chemoattractant protein-1
MDM	monocyte-derived macrophage
MHC-II	major histocompatibility complex II
MMP	matrix metalloproteinase
MMP-2	matrix metalloproteinase-2
MMP-9	matrix metalloproteinase-9
NADPH	nicotinamide adenine dinucleotide phosphate
NF- $\kappa$ B	nuclear factor kappa-light-chain-enhancer of activated B cells
NOS	nitric oxide synthase
NLR	NOD-like receptor
NLRP-3	NOD-like receptor family, pyrin domain containing 3
OGD	oxygen-glucose deprivation
PAMP	pathogen-associated molecular pattern
ROS	reactive oxygen species
SEM	standard error of the mean
TGF- $\beta$	transforming growth factor beta
Th1	T-helper type 1
Th2	T-helper type 2
TLR	toll-like receptor
TLR-4	toll-like receptor 4

tMCAO	transient middle cerebral artery occlusion
TNF	tumor necrosis factor
Tregs	regulatory T-cells
VCAM-1	vascular cell adhesion molecule-1

## INTRODUCTION

Stroke is a neurological disease with high mortality and morbidity rates. In 2015, the stroke death rate was 73.3 deaths in every 100,000 stroke patients in the United States (Yang, 2017). It is the fifth leading cause of death in the United States and is globally the second most common cause of death (Benjamin et al., 2017). Each year, there are around 800,000 occurrences of stroke worldwide in the United States (Benjamin et al., 2017). Stroke is also significantly detrimental to one's quality of life; many stroke survivors suffer from long-term complications, including motor and cognitive deficits (Lawrence et al., 2001). Around 60% of stroke-survivors experience an impairment in manual dexterity, or the loss of the ability to perform coordinated and fine movements with their hands 6 months after stroke (Claflin, Krishnan, & Khot, 2015). Additionally, the percentage of stroke survivors suffering from post-stroke dementia can range anywhere from 20% to 80% depending on the country, the population and question, and the cognitive tests used for evaluation (Sun, Tan, & Yu, 2014).

Stroke is the sudden death of brain tissue due to the lack of oxygen and can be broadly divided into two different types, ischemic stroke and hemorrhagic stroke. Hemorrhagic stroke occurs when there is a rupture in a blood vessel in the brain (Caplan, Kasner, & Dashe, 2017). It can be further subdivided into a intracerebral hemorrhage, bleeding within the brain tissue, or a subarachnoid hemorrhage, bleeding within the subarachnoid space (Caplan et al., 2017). On the other hand, ischemic stroke occurs due

to a lack of blood perfusion to the brain, which can be caused by different factors including thrombosis, embolism, lacunar infarction, or systemic hypoperfusion, and leads to neural tissue necrosis (Caplan et al., 2017; Giraldo, 2017). The middle cerebral artery (MCA) is one of the largest arteries in the brain and is the most common blood vessels involved in ischemic stroke (Slater, 2018). Hemorrhagic stroke is shown to have a higher mortality rate compared to ischemic stroke (Andersen, Olsen, Dehlendorff, & Kammersgaard, 2009). However, hemorrhagic stroke composes 32% of all strokes while ischemic stroke composes 68% (Caplan et al., 2017). There are many different non-modifiable and modifiable risk factors associated with stroke that have been identified. Non-modifiable risk factors include genetic predisposition, aging, and ethnicity, while modifiable risk factors include hypertension, diabetes, lack of physical activity, smoking, and obesity. (Meschia et al., 2014)

### **Obesity as an epidemic and risk factor for stroke**

Obesity, defined as a body mass index (BMI) of 30 or higher, has been a rising global epidemic over the past three decades, during which the prevalence of obesity approximately doubled for adults between 1980 and 2008 (World Health Organization, 2018a). In 2016 worldwide, 39% of people of at least 18 years of age are overweight (defined as having a BMI between 25 and 30) and 13% are obese (World Health Organization, 2018b). Obesity is currently still a major problem, as more than 2.8 million people worldwide die as a result of being overweight or obese every year (U.S Department of Health and Human Services, 2018).

People who are overweight or obese are more likely to have an ischemic stroke compared to those of normal weight (Guo et al., 2016; Mitchell et al., 2015; Strazzullo et al., 2010; Suk et al., 2003). In one meta-analysis, it was found that an overweight person is 1.22 times more likely than a person of normal weight to have an ischemic stroke, while an obese person is 1.64 more likely to have an ischemic stroke compared to a person of normal weight (Strazzullo et al., 2010). Another study demonstrates that people who are overweight in young adulthood are 1.36 times more likely than people of normal weight to have a stroke while those who are obese in young adulthood are 1.81 times more likely to have stroke compared to those of normal weight (Guo et al., 2016).

### **Pathophysiology of obesity**

Adipose tissue was traditionally thought to act mostly as a storage site for triglycerides (Greenberg & Obin, 2006). However, the discovery that adipose tissue secretes different signaling proteins, particularly the discovery of leptin in 1994 (Y. Zhang et al., 1994), led researchers to conceptualize adipose tissue as an “endocrine organ” (Greenberg & Obin, 2006). There are more than 50 signaling proteins, including adipose-specific and non-specific proteins, known to be released from adipose tissue, which are collectively called adipokines (Trayhurn & Wood, 2004). Adipokines play functional roles in different physiological processes including appetite regulation, metabolism, angiogenesis, immunity, and inflammation (Trayhurn & Wood, 2004). For example, the adipokine leptin acts on leptin receptors in the hypothalamus, decreasing appetite and increasing energy expenditure (Halaas et al., 1995; Lee et al., 1996). Another

major adipokine released by adipocytes is adiponectin, which upregulates fatty acid oxidation in tissues such as skeletal muscles and increases insulin sensitivity (Fruebis et al., 2001; Yamauchi et al., 2001).

Besides adipocytes, adipose tissue consists of different cell types including fibroblasts and immune cells (Huh, Park, Ham, & Kim, 2014). The immune response consists of the innate immune response and the adaptive immune response. The innate immune system is the first to respond to infection or injury and consists of the rapid activation of immune cells such as macrophages, neutrophils, dendritic cells, mast cells and innate lymphoid cells (Abbas, Lichtman, & Pillai, 2016d). While the innate immune response is immediate, it only provides non-specific defense and responds to biomolecules generally shared by microbes called pathogen-associated molecular patterns (PAMPs) or biomolecules that are released by cells during cell death, called damage-associated molecular patterns (DAMPs) (Abbas et al., 2016d). In contrast, the adaptive immune system activates more slowly but provides a more specific response. The adaptive immune system consists of B and T-cells, which develop to recognize and target specific antigens (Abbas, Lichtman, & Pillai, 2016e). It is important to note that the two components of the immune system are highly interactive with each other. For example, the innate dendritic cells and macrophages are also antigen-presenting cells (APCs), which are cells that possess and use a surface molecule called the major histocompatibility complex II (MHC-II) to activate T-cells and trigger them to adapt different phenotypes (Abbas, Lichtman, & Pillai, 2016a).

A variety of studies confirm that obese adipose tissues adapt a pro-inflammatory phenotype. Obese adipose tissue exhibits an upregulation of tumor necrosis factor (TNF), interleukin-6 (IL-6), monocyte chemoattractant protein-1 (MCP-1), along with other pro-inflammatory mediators, and importantly some of these contribute to metabolic pathologies including insulin insensitivity (Fried, Bunkin, & Greenberg, 1998; Hotamisligil, Shargill, & Spiegelman, 1993; Sartipy & Loskutoff, 2003). One study found that the number of macrophages is positively correlated with the size of adipocytes and the BMI of patients, likely due to the infiltration of circulating monocytes, which differentiate into macrophages within the adipose tissue (Weisberg et al., 2003). Increased secretion of MCP-1 along with other cytokines from adipocytes are responsible for this macrophage infiltration (Kanda et al., 2006). Macrophages that reside in adipose tissue also release pro-inflammatory mediators such as TNF, IL-6, and inducible nitric oxide synthase (iNOS) (Weisberg et al., 2003). Together, an increase in the number of macrophages and their differentiation into a more pro-inflammatory state leads to this chronic low-grade inflammation in the obese.

The inflammasomes, a protein complex responsible for activating a pro-inflammatory response, also play a role in obesity-induced inflammation. NOD-like receptor family pyrin domain containing 3 (NLRP3), a type of Nod-like receptor (NLR), activates caspase-1, which upregulates production of pro-inflammatory cytokines including interleukin-1 $\beta$  (IL-1 $\beta$ ) (Abbas et al., 2016d). Studies found activation of NLRP3 and caspase-1 in obese adipose tissues, in association with increasing IL-1 $\beta$  and interleukin-18 (IL-18) production and secretion (Stienstra et al., 2010, 2011;

Vandanmagsar et al., 2011). Deletion of NLRP3 or caspase-1 in obese adipose tissue results in increased glucose transporter type 4 (GLUT-4) and adiponectin, which leads to increased insulin sensitivity (Stienstra et al., 2010). Furthermore, evidence shows that disruption of inflammasome activation results in reduced MCP-1 production from adipose tissue, reduced macrophage infiltration, decreased adipocyte size, and increased rates of fat oxidation (Stienstra et al., 2010, 2011). The transcription factor called nuclear factor kappa-light-chain-enhancer of activated B cells (NF- $\kappa$ B), is also involved in the obesity-induced inflammatory response. Interestingly, free fatty acids (FFAs) are able to act through toll-like receptor 4 (TLR-4) on macrophages and adipocytes, which then promotes NF- $\kappa$ B signaling, causing increased inflammation and decreased glucose tolerance (Shi et al., 2006).

In contrast to obese adipose tissue, lean adipose tissue tends to exhibit an anti-inflammatory phenotype. For example, the majority of the macrophage population in lean adipose tissue secretes anti-inflammatory cytokines such as IL-10, which helps improve insulin sensitivity (Lumeng, Bodzin, & Saltiel, 2007). It is known that the cytokines interleukin-13 (IL-13) and interleukin-4 (IL-4) trigger alternative activation of macrophages into this anti-inflammatory phenotype. While adipocytes themselves can secrete IL-13 and IL-4 (Kang et al., 2008), a study by Wu et al. (2011) found that the majority of IL-4 within the adipose tissue is secreted from eosinophils, a type of innate leukocyte (Wu et al., 2011). The secretion of interleukin-5 (IL-5), a cytokine released by innate lymphoid type 2 cells resident to adipose tissue, is one proposed signaling

mechanism of signaling to facilitate the infiltration of eosinophils into adipose tissue (Molofsky et al., 2013).

In addition to the differences in number and phenotype of innate immune cells between obese and lean adipose tissue, there are also differences in the composition and phenotype of adaptive immune cells like T-lymphocytes, also known as T-cells. IL-4 secreted by eosinophils can also cause T-cells to differentiate into T-helper type 2 (Th2) CD4<sup>+</sup> cells, which can secrete additional IL-4 and IL-13, further inducing macrophages to adopt an anti-inflammatory phenotype (Abbas, Lichtman, & Pillai, 2016b). This may be one reason that lean visceral adipose tissue has a higher proportion of Th2 CD4<sup>+</sup> cells compared to the proportion in obese visceral adipose tissue (S. Winer et al., 2009). The study by Winer et al. (2009) showed that the number of CD4<sup>+</sup> Foxp3<sup>+</sup> regulatory T-cells (Tregs), another subpopulation of T-cells which secretes IL-4, IL-10, and IL-13 (Tiemessen et al., 2007), are increased in lean but not in obese adipose tissue, leading to an anti-inflammatory environment (S. Winer et al., 2009). This study also demonstrated that obese adipose tissue tends to have fewer CD4<sup>+</sup> Foxp3<sup>+</sup> Tregs than CD4<sup>+</sup> T-helper type 1 (Th1) CD4<sup>+</sup> cells (S. Winer et al., 2009). Th1 cells are a pro-inflammatory subtype of T-cells which release the interferon- $\gamma$  (IFN- $\gamma$ ), a cytokine that activates a pro-inflammatory macrophage response (Abbas et al., 2016b). There is also evidence that CD8<sup>+</sup> cytotoxic T-cells contribute to the inflammatory response in obesity, as CD8<sup>+</sup> cytotoxic T-cells are known to help activate macrophages (Abbas et al., 2016d). One study showed that CD8<sup>+</sup> cytotoxic T-cells infiltrate adipose tissue in animals fed high-fat

diet (HFD) and that these cells recruit and activate infiltrating macrophages, ultimately contributing to insulin resistance (Nishimura et al., 2009).

In addition to T-cells, B-lymphocytes, also called B-cells, are a type of adaptive immune cell shown to modulate the inflammatory phenotype in adipose tissue. A study by Winer et al. (2011) shows that B-lymphocytes infiltrate into adipose tissue following diet-induced obesity and undergo isotype switching to produce pathogenic immunoglobulin Gs (IgGs), which causes macrophages within adipose tissue to secrete TNF through a mechanism involving the fragment crystallizable region of immunoglobulins (D. A. Winer et al., 2011). Interestingly, this study also suggests that B-cells activate T cells in a major histocompatibility complex-dependent manner, possibly allowing CD8<sup>+</sup> cytotoxic T-cells and CD4<sup>+</sup> T-cells to produce IFN- $\gamma$ , which in turn possibly leads to insulin resistance (D. A. Winer et al., 2011). Like T-cells, B-cells also have an alternative regulatory phenotype, called regulatory B-cells (Bregs). A study by Nishimura et al. (2013) found that a unique subpopulation of Bregs specifically residing in lean adipose tissue is one of the main sources of the anti-inflammatory cytokine IL-10 expressed in adipose tissue (Nishimura et al., 2013). The same study demonstrated that knocking out the B-cell specific IL-10 gene increased numbers of CD8<sup>+</sup> cytotoxic T-cells and pro-inflammatory macrophages and decreased insulin sensitivity in obese adipose tissue (Nishimura et al., 2013). A study by Wang et al. (2014) showed that one mechanism of inducing this Breg phenotype is through interleukin-35 (IL-35) signaling (R.-X. Wang et al., 2014).

In summary, multiple studies demonstrate that obesity induces inflammation response in adipose tissue, and that this leads to insulin resistance and other metabolic pathologies. Inflammation in obese adipose tissue is characterized by higher levels of Th1 CD4<sup>+</sup> cells, pathogenic IgG-producing B-cells, pro-inflammatory macrophages accompanied by the decrease in Th2 CD4<sup>+</sup> cells, CD4<sup>+</sup> Foxp3<sup>+</sup> Tregs, and Bregs. Pro-inflammatory mediators that have been causally implicated in insulin resistance include the inflammasome and TNF. On the other hand, the anti-inflammatory cytokine IL-10 directly antagonizes the detrimental effects of TNF on insulin signaling, leading to better glucose tolerance (Lumeng et al., 2007). In addition, the results from these studies show that the innate and adaptive immune response affect each other, leading to an overall pro-inflammatory or anti-inflammatory environment in adipose tissue. For example, eosinophils secrete IL-4 which causes T-cells to differentiate into Th2 CD4<sup>+</sup> cells and secrete further anti-inflammatory cytokines. Meanwhile, Th1 CD4<sup>+</sup> cells secrete IFN- $\gamma$ , a pro-inflammatory cytokine that causes macrophages to produce more pro-inflammatory mediators.

### **Neuroinflammatory response following stroke**

In addition to responding to infections and invading pathological microorganisms in the human body, the innate immune system also responds when tissue is damaged in stroke. One group of receptors that play a part in activating this innate immune response is the toll-like receptors (TLRs) (Abbas et al., 2016d). Microglia, the resident macrophages of the central nervous system (CNS), are known to possess TLRs 1-9

(Olson & Miller, 2004), which can each respond to different ligands and DAMPs, including those released from damaged blood vessels, extracellular matrix (ECM), and necrotic cells (Karikó, Weissman, & Welsh, 2004). For example, mRNA released from necrotic cells can bind to and activate TLR 3 (Karikó, Ni, Capodici, Lamphier, & Weissman, 2004) while fibronectin, a component found in the ECM binds and activate TLR 4 (Okamura et al., 2001). Other DAMPs released during cell death include high mobility group box-1, heat shock proteins, and low-density lipoprotein (Famakin, 2014). TLR activation leads to signaling cascades that activate transcription factors such as NF- $\kappa$ B and interferon regulator factors (IRFs), which cause increased expression of pro-inflammatory cytokines and adhesion molecules (Abbas et al., 2016d). Inflammasomes such as NLRP3 are also involved in innate immunity by upregulating pro-inflammatory cytokines and respond to tissue death through sensing substances that indicate cellular death such as extracellular adenosine triphosphate (ATP) and uric acid crystals derived from nucleic acids (Abbas et al., 2016d).

As mentioned above, microglia are the resident macrophages of the CNS. They have a variety of functions in the normal brain including synaptic remodeling, clearing debris, and constantly surveying their environment through dynamic movements of their ramified processes (Nimmerjahn, Kirchhoff, & Helmchen, 2005; Patel, Ritzel, McCullough, & Liu, 2013). Microglia response to CNS damage caused by stroke in the acute phase of neuroinflammation, which is loosely defined as the relatively immediate time period after the occurrence of stroke. In fact, they become activated as early as 2 hours after the onset of ischemic stroke (Kawabori & Yenari, 2015). As mentioned

earlier, one possible mechanism of microglia activation is through the DAMP pathway, where DAMPs released by necrotic cells can bind to TLRs on microglia and initiate cellular changes (Patel et al., 2013). Microglia in the injured brain are also able to sense extracellular ATP released from damaged cells. In response, they extend and move their processes towards the injured site and form a barrier between damaged and normal tissue (Davalos et al., 2005). In addition, microglia are shown to actively undergo cellular division after an ischemic stroke, leading to increased numbers of microglia in the areas surrounding the infarct core (T. Li et al., 2013). Overall, the activation, proliferation, and overall “intense reaction” of microglia is called “microgliosis” (T. Li & Zhang, 2016).

Like peripheral macrophages, microglia can adopt a more pro-inflammatory or anti-inflammatory phenotype. Microglia are known to release anti-inflammatory cytokines such as IL-10, IL-4, and transforming growth factor- $\beta$  (TGF- $\beta$ ), which helps with tissue repair and neuroprotection (Patel et al., 2013). In contrast, microglia can also release pro-inflammatory cytokines like TNF, IL-1 $\beta$ , IFN- $\gamma$ , and IL-6 as well as other pro-inflammatory molecules like matrix metalloproteinases (MMPs), reactive oxygen species (ROS) and nitric oxide synthase (NOS), which further exacerbates the neuroinflammatory response (Patel et al., 2013). A study by Gregersen et al. (2000) shows that microglia and infiltrating monocyte-derived macrophages (MDMs) are responsible for the elevated levels of TNF seen early after stroke, which peak at 12 hours after middle cerebral artery occlusion (MCAO), a common ischemic stroke model used in animals (Gregersen, Lambertsen, & Finsen, 2000). One study by Hu et al. (2012) found that microglia and infiltrating macrophages secrete anti-inflammatory cytokines like

TGF- $\beta$  and IL-10 at 1 to 3 days after MCAO, and that microglia and infiltrating macrophages start expressing pro-inflammatory mediators such as iNOS from day 3 and onwards (Hu et al., 2012). Other studies in different CNS injury models have also supported a transition from a more anti-inflammatory to a more pro-inflammatory phenotype in microglia and peripheral macrophages (Hu et al., 2015).

Astrocytes, another type of glial cell, also undergo functional and physical changes during the acute phase of neuroinflammation. Astrocytes are normally responsible for a number of roles in the CNS, including guiding neuronal development, regulating neurotransmitter metabolism, maintaining synapses, and maintaining the blood brain barrier (BBB) (Dong & Benveniste, 2001). The BBB is a tightly regulated barrier that helps prevent changes in plasma composition from affecting brain function (Abbott, 2002). Like microglia, astrocytes also undergo a number of changes in response to brain ischemic injury, such as increased swelling (Garcia, Kalimo, Kamijyo, & Trump, 1977), increased calcium ion signaling, and upregulation of glial fibrillary acidic protein (GFAP), an intermediate filaments protein expressed by astrocytes (Choudhury & Ding, 2016). In addition to the change from a normal astrocyte phenotype to a reactive astrocyte phenotype during brain ischemic injury, there is proliferation of astrocytes (Panickar & Norenberg, 2005) and later on, the formation of a glial scar in the penumbra around the stroke core, separating healthy tissue from damaged tissue (Choudhury & Ding, 2016). It is known that this glial scar formed by astrocytes undergoes remodeling and persists during the chronic phase and beyond after stroke (Burda & Sofroniew,

2014). These phenotypical changes and reactions by astrocytes to brain injury are termed “astrogliosis”.

Astrocytes also play a prominent role in the acute immune response after stroke. Like microglia, astrocytes also express TLRs (Farina, Aloisi, & Meinl, 2007), and can respond to DAMPs and other ligands released from damaged tissue after stroke. Astrocytes can interact with and activate microglia and other infiltrating cells in the CNS after ischemic stroke. For example, astrocytes can release ATP which in turn activates microglia (Takano, Oberheim, Cotrina, & Nedergaard, 2009). A study by Inose et al. (2015) also found that astrocytes can release the molecule lysophosphatidylcholine, which induces expression of the pro-inflammatory mediators MCP-1 and its receptor C-C chemokine receptor type 2 (CCR-2) in microglia after ischemic stroke (Inose, Kato, Kitagawa, Uchiyama, & Shibata, 2015). Furthermore, another study by Che et al. (2001) suggests that astrocytes themselves also produce and release MCP-1 (Che, Ye, Panga, Wu, & Yang, 2001). Astrocytes are also known to be APCs and therefore express MHC-II, meaning they are capable of activating T-cells in the CNS (Dong & Benveniste, 2001), therefore playing a role in priming the adaptive immune response. Together, these studies show that astrocytes play a role in both innate and adaptive immunity in the CNS.

Different studies suggest that astrocytes play a neuroprotective role after stroke. A study by Nawashiro et al. (2000) shows that mice lacking glial fibrillary acid protein (GFAP), which is upregulated by astrocytes during astrogliosis, have larger infarcts and decreased cortical cerebral blood flow after MCAO and tMCAO compared to those found in wild type mice (Nawashiro, Brenner, Fukui, Shima, & Hallenbeck, 2000). This

suggests that GFAP in astrocytes helps attenuate the progress of further brain damaged initiated by ischemic stroke (Nawashiro et al., 2000). Another study done by Hayakawa et al. (2010) suggested that astrocytes also contribute to neurovascular remodeling and improves motor functioning after ischemic stroke in mice (Hayakawa et al., 2010). By inhibiting the metabolism in astrocytes 5 days after onset of ischemic stroke, mice have worst neurovascular remodeling and motor functioning compared to those with uninhibited astrogliosis (Hayakawa et al., 2010).

While the studies mentioned above showcase the beneficial effects of astrocytes, there are other studies that demonstrate that they can have detrimental effects. A study by Wang et al. (2008) demonstrated that astrogliosis after MCAO in rats is closely associated with neuronal death and that inhibiting astrocyte proliferation that occurs during astrogliosis after MCAO decreases this neuronal death (W. Wang et al., 2008). In addition, a study by Dvorianchikova et al. (2009) suggests that inhibiting NF- $\kappa$ B signaling in astrocytes after ischemic injury decreases the levels of pro-inflammatory mediators such as ICAM-1, VCAM-1, MCP-1, TNF, and NOS and increases the survival of neurons within the injured region (Dvorianchikova et al., 2009). A recent study by Liddel et al. (2017) even found that microglia are able to induce a subpopulation of reactive astrocytes called “A1 astrocytes”, which then induces the death of neurons and oligodendrocytes (Liddel et al., 2017).

As mentioned earlier, both microglia and astrocytes secrete pro-inflammatory cytokines and chemokines, which recruit other innate immune cells into infarct area (Benveniste, 1997; J. Y. Kim, Park, Chang, Kim, & Lee, 2016). Chemokines such as

MCP-1 and cytokine-induced neutrophil chemoattractant (CINC) help recruit monocytes and neutrophils to the site of injury, respectively (Huang, Upadhyay, & Tamargo, 2006). Pro-inflammatory cytokines such as TNF and interleukin-1 (IL-1) induce endothelial cells of the cerebral microvasculature to upregulate adhesion molecules including E-selectins, P-selectins, intercellular adhesion molecule-1 (ICAM-1), and vascular cell adhesion molecule-1 (VCAM-1), which allow innate immune cells such as neutrophils and monocytes from the systemic circulation to bind to the endothelium of these blood vessels and infiltrate into the injured brain tissue (Abbas et al., 2016d; Stanimirovic, Wong, Shapiro, & Durkin, 1997; R. Zhang, Chopp, Zhang, Jiang, & Powers, 1998).

In addition to homeostatic regulation of the environment in the brain (Abbott, 2002), the BBB is also important for restricting peripheral immune cells from entering the CNS (Muldoon et al., 2013). However, the BBB increases in permeability early after stroke, contributing to neuroinflammation. An early study by Rosenberg et al. (1998) found that the BBB increased its permeability at two time points, at 3 hours and 48 hours after a transient middle cerebral artery occlusion (tMCAO), an animal model of ischemic stroke where the MCA is only temporarily occluded (Rosenberg, Estrada, & Dencoff, 1998; Turner & Sharp, 2016). The permeability of the BBB then later went back to normal levels by 14 days after tMCAO (Rosenberg et al., 1998; Turner & Sharp, 2016). The increased BBB permeability seen at 3 hours after tMCAO is associated with increased levels of MMP-2 (matrix metalloproteinase-2) and the increased permeability seen after 48 hours was associated with increased levels of MMP-9 (matrix metalloproteinase-9) (Rosenberg et al., 1998; Turner & Sharp, 2016). Both of these

enzymes contribute to the breakdown of extracellular matrix components of the cerebral vasculature and it is shown that neutrophils may be a major contributor to the increased levels of MMP-9 after stroke (Huang et al., 2006; Justicia et al., 2003; Turner & Sharp, 2016). This opening of the BBB soon after stroke is associated with increased infiltration of peripheral immune cells into the injured brain (Turner & Sharp, 2016). In addition, the increased BBB permeability is also associated with edema in the same hemisphere where the stroke occurred (Bralet, Beley, Beley, & Bralet, 1979).

Although the timing of the infiltration of systemic immune cells into the brain may vary between different stroke models, species, and studies, the first responders of ischemic stroke from the peripheral circulation generally include monocytes and neutrophils, both of which are part of the innate immune system (Chu et al., 2014; Famakin, 2014; Gelderblom et al., 2009; Grønberg, Johansen, Kristiansen, & Hasseldam, 2013; Hallenbeck et al., 1986; Schroeter, Jander, Witte, & Stoll, 1994).

Neutrophils, a type of granulocyte, develop in the bone marrow and can respond to damaged tissue by infiltrating into the site of injury and phagocytosing necrotic tissue, although their life span is only a few hours once in the extravascular tissue (Abbas et al., 2016d). Studies show that neutrophils start infiltrating into the injured hemisphere of the brain as early as 1 to 3 hours after stroke, with peak levels of infiltration at 1 to 3 days after stroke, although these studies have variations between the time of onset of infiltration, based on the stroke model (Famakin, 2014; Grønberg et al., 2013; Hallenbeck et al., 1986). To reach to the site of injury, neutrophils exocytose granules containing proteases including elastases, collagenases, and gelatinases (such as MMP-9), which

facilitate the breakdown components of the ECM (Turner & Sharp, 2016). It is thought that the BBB breakdown and release of proteases and ROS by neutrophils can possibly contribute to more tissue damage, but neutrophils may also contribute to beneficial effects such as vascular remodeling and angiogenesis after stroke (Jickling et al., 2015).

Like neutrophils, monocytes are made in the bone marrow and recruited early on after stroke (Abbas et al., 2016d). Once monocytes are recruited into the target tissue, they can then differentiate into macrophages, which tend to survive longer in the brain than neutrophils (Abbas et al., 2016d). MDMs are observed in the injured hemisphere as early as 12 hours after stroke and have a peak response at days 3 and 7 after stroke (Gelderblom et al., 2009; Grønberg et al., 2013). Since microglia are CNS-specific macrophages that populate the CNS during embryonic development (Abbas et al., 2016d), they have many similar phenotypes to peripheral macrophages, which makes them difficult to distinguish from each other (Patel et al., 2013). For example, the cell marker CD68 is found on both microglia and peripheral macrophages. As such, the extent to which infiltrating macrophages contribute to microgliosis is still being debated (Greter, Lelios, & Croxford, 2015; T. Li et al., 2013). Like microglia, infiltrating macrophages likely polarize into pro-inflammatory or anti-inflammatory phenotypes, allowing them to phagocytose necrotic tissue and perpetuate neuroinflammation or become involved with tissue repair (Abbas et al., 2016d).

Although peripheral macrophages are thought to be the earlier responders after stroke, there are studies showing that they can infiltrate into the infarct core after the acute phase. By labeling peripheral macrophages with fluorine-19, Vindegaard et al.

(2017) demonstrated that the number of infiltrating peripheral macrophages actually peaks at 14 days in the infarct area after MCAO, and that there continue to be high numbers in this area even at 28 days after MCAO (Vindegaard et al., 2017). Another study performed by Doyle et al. (2015) showed increased numbers of peripheral macrophages and/or microglia in the infarct core of mice at 7 weeks after middle cerebral artery occlusion with hypoxia (DH) stroke, an ischemic stroke model where the distal portion of the MCA is occluded and the animal is further subjected to hypoxia, and that these cells possibly contribute to a larger adaptive immune response that worsens stroke outcomes (Doyle et al., 2015). It is important note that the increased CD68 expression in the stroke core in this study by Doyle et al. (2015) may also represent the proliferation of microglia or their migration from other parts of the brain, in addition to increased infiltration or proliferation of peripheral macrophages.

Many studies show that the pro-inflammatory mediators released by microglia and peripheral macrophages contribute to larger brain damage after stroke. In a study by Giulian et al. (1993), the immunosuppression of both microglia and macrophages with chloroquine and colchicine, which are both known to be macrophage suppressors, 1 hour after tMCAO in rats resulted in lower amounts of neurotoxic compounds, possibly leading to higher rates of neuron survival (Giulian, Corpuz, Chapman, Mansouri, & Robertson, 1993). Another study by Chen et al. (2009) showed that inhibiting Nicotinamide adenine dinucleotide phosphate (NADPH) oxidase in mice, which is expressed in microglia and is a responsible for producing ROS, resulted in a 50% decrease in the infarct area after MCAO compared to the infarct areas in mice without

NADPH oxidase inhibition (Chen, Song, & Chan, 2009). Microglia are also a source for MMPs (Kawabori & Yenari, 2015) and a study by Asahi et al. (2000) showed that knocking out the MMP-9 gene or inhibiting its enzymatic activity in mice after ischemic injury reduces the lesion size (Asahi et al., 2000). These studies show the detrimental effects microglia and macrophages can exert on neural tissue after ischemic stroke.

However, there is also evidence that macrophages can be neuroprotective in ischemia. A study by Neumann et al. (2006) showed that the application of microglia to rat hippocampal sections at 24 hours before oxygen-glucose deprivation (OGD), another model of ischemic injury, protected neurons from OGD-induced damage (Neumann et al., 2006). This study further showed that microglia with downregulated CD11a, which is involved in cellular adhesion, fails to provide protection against OGD-induced damage, suggesting that adhesion of microglia to neurons after OGD is a mechanism involved in neuroprotection (Neumann et al., 2006). Another study by Imai et al. (2007) found that intravenous injection of cultured microglia as late as 24 hours after global forebrain ischemia in gerbils resulted in decreased damage to neurons (Imai et al., 2007). Furthermore, microglia-treated animals had normal memory performance and increased neurotrophic factors like brain-derived neurotrophic factors and glia cell-derived neurotrophic factor, which contributes to the survival of neurons (Imai et al., 2007).

There is evidence that T-cells are involved in the immunological pathology of ischemic stroke, although their involvement is not as well studied as those of other leukocytes (Arumugam, Granger, & Mattson, 2005). An early study done by Jander et al. (1995) shows that T-cells can adhere to cortical vasculature between 1 to 2 days after

ischemic stroke in rats and that there are increased numbers of T-cells by 3 days in the area surrounding the infarct core (Jander, Kraemer, Schroeter, Witte, & Stoll, 1995). A study by Stevens et al. (2002) using flow cytometry also verifies this increased T-cell levels at 3 days after ischemic stroke (Stevens et al., 2002).

T-cells are involved in the chronic phase after ischemic stroke, which is loosely defined as weeks after the onset of stroke. From labeling peripheral lymphocytes, Feng et al. (2017) found that lymphocyte infiltration is seen even 14 days after ischemic stroke models in mice, including CD4<sup>+</sup> T-cells, CD8<sup>+</sup> T-cells, as well as natural killer T-cells (Feng et al., 2017). This time point after stroke corresponds with increased expression of ROS and inflammatory cytokines like IFN- $\gamma$  and TNF (Feng et al., 2017). Vindegaard et al. (2017) even demonstrated a significant increase in T-cell numbers 28 days after MCAO in mice (Vindegaard et al., 2017). Studies suggest that T-cells exacerbate the neuroinflammation response after ischemic stroke and leads to worse stroke outcomes. A study by Kleinschnitz et al. (2010) showed that mice lacking mature T and B cells have reduced infarct volumes after tMCAO compared to wild type mice, but administering T-cells into mature T and B-cell null mice results in infarct sizes and motor functional deficits similar to those found in wild type (Kleinschnitz et al., 2010).

On the other hand, it is also demonstrated that different subtypes of T-cells play different roles after stroke. As described above, the CD4<sup>+</sup> T-cell population can be further divided into different cell subpopulation, including Th1, Th2, and Th17 cells, based on the cytokines it produces and its ability to activate different cell types (Abbas et al., 2016b). Th1 CD4<sup>+</sup> cells are able to release IFN- $\gamma$  and able to polarize macrophages into

the M1 phenotype (Abbas et al., 2016b). They can also activate microglia, increase vascular permeability, and increase major histocompatibility complex I expression, further exacerbating the inflammatory response (Arumugam et al., 2005). Th17 CD4+ cells are known to contribute to the inflammatory response by producing pro-inflammatory cytokines such as interleukin-22 (IL-22) (Stockinger, Veldhoen, & Martin, 2007). On the other hand, Th2 CD4+ cells are able to secrete anti-inflammatory cytokines including IL-4, IL-10, and IL-13 (Abbas et al., 2016b). Note that these different T-cell subtypes are also involved in a variety of pathophysiological states besides stroke, as seen earlier in chronic obesity.

It is thought that these different subpopulations of CD4+ T-cells may each play a unique role in promoting or inhibiting the neuroinflammatory response after ischemic stroke. The study by Gu et al. (2012), one of the few studies that looked at the neuroinflammatory roles of different CD4+ T-cell subtypes after stroke, found that Th2 CD4+ T-cell- deficient mice have larger infarct sizes and worst neurological deficits while mice deficient in Th1 CD4+ T-cells have smaller infarct sizes and less neurological deficits compared to wild type mice after ischemic stroke (Gu et al., 2012). This study also found an increase in neutrophil and macrophage activity 2 days after stroke in Th2 CD4+ T-cell deficient mice while the activities of these cells decreased in Th1 CD4+ T-cell deficient mice (Gu et al., 2012). Furthermore, they also found *in vitro* that Th1 CD4+ T-cell deficiency leads to lesser neuronal death, while Th2 CD4+ T-cell deficiency causes more neuronal death (Gu et al., 2012). These results are expected, since Th1

CD4+ T-cells are shown to be pro-inflammatory while Th2 CD4+ T-cells have anti-inflammatory properties.

There are also studies that attempt to understand the different possible mechanism that T-cells may use to worsen neuroinflammation after stroke. A recent study by Zhao et al. (2018) suggests that first apoptosis signal receptor ligand (FasL) on CD4+ cells promote microglia to adopt an pro-inflammatory phenotype via the NF- $\kappa$ B pathway after ischemic stroke (Zhao et al., 2018). Brait et al. (2010) showed that T-cells can contain NADPH oxidase 2, which contributes to the increased levels of superoxides after ischemic stroke in male mice models, suggesting another mechanism that T-cells may use to contribute to neural injury (Brait et al., 2010).

Like T-cells, B-cells are also thought to be the late responders in the neuroinflammatory response after stroke. While T-cells also respond during the acute phase after stroke, there is a disagreement in the literature as to whether B-cells are involved in the acute phase. Several studies found that B-cells most likely do not play a major role during the acute phase. Schumann et al. (2017) reported that B-cell deficient mice had similar infarct sizes to those in control mice at day 1 and 3 after tMCAO (Schuhmann, Langhauser, Kraft, & Kleinschnitz, 2017). In this study, B-cell deficient mice had similar numbers of monocytes and neutrophils in the ipsilateral hemisphere compared to control mice (Schuhmann et al., 2017). Additionally, there was also no difference in the amount of neuronal apoptosis, the degree of astrogliosis, or the levels of TNF and IL-1 $\beta$  between these two groups (Schuhmann et al., 2017). A study by Kleinschnitz et al. (2010) found that reconstituting B-cells in T and B-cell deficient mice

does not significantly change the infarct size compared to that of T and B-cell deficient mice 24 hours after tMCAO, further suggesting that B-cells do not contribute to the damage found at this time point (Kleinschnitz et al., 2010).

In contrast with these studies, Ren et al. (2011) demonstrated that B-cell deficient mice had larger infarct sizes and more severe sensorimotor deficits at 48 hours after 60 min. of tMCAO, accompanied with increased numbers of neutrophils, T-cells, and macrophages in the ipsilateral hemisphere (Ren et al., 2011). It was further found that restoring B-cells in B-cell deficit mice eliminated these affects from tMCAO, but transferring IL-10 deficient B-cells into B-cell deficient mice did not reduce infarct size or improve neurological functioning (Ren et al., 2011). Overall, this study suggests that B-cells exert neuroprotective effects early after stroke by producing IL-10.

Doyle et al. (2015) reported that B-cells are rarely found in coronal sections of mice brain 1 week after DH stroke (Doyle et al., 2015). However, B-cells are observed in the stroke core in the chronic phase at 7 weeks after DH stroke and even at 12 weeks after DH stroke (Doyle et al., 2015). In addition, these B-cells are in close proximity to dendritic cells and T-cells, and 9% of the B-cells in the stroke core at 7 weeks after dMCAO matured into antibody-synthesizing plasma cells (Doyle et al., 2015). This is not surprising, as dendritic cells and CD4<sup>+</sup> T-cells are crucial for presenting antigens to B-cells for activation and for providing proliferation and isotype switching signals (Abbas, Lichtman, & Pillai, 2016c; Wykes & Macpherson, 2000). Furthermore, the large number of B-cells in the stroke core at 7 weeks after DH stroke in mice corresponds with an onset of cognitive deficits, which is measured by two tasks that both assess cognition (Doyle et

al., 2015). At this time point, these mice also developed a deficit in long-term potentiation (LTP) in the hippocampus, which is an electrophysiological correlate of memory (Doyle et al., 2015).

Interestingly, Doyle et al. (2015), also reported that the levels of IgG1, IgG2, and IgA antibodies were elevated in adjacent brain regions 7 weeks after stroke compared to sham animals, and that there is a significant increase in IgA levels between week 1 and 7 after stroke, suggesting that B-cells had undergone both IgG and IgA isotype switching between week 1 and 7 after stroke (Doyle et al., 2015). The authors speculated that the antibodies produced by these B-lymphocytes might activate Fc receptors, mediate complement protein activation, or target host tissue in an autoreactive fashion, contributing to the neurological dysfunction observed at 7-weeks after stroke (Doyle et al., 2015). To further confirm that this delayed-cognitive deficit is due to B-cells found in the stroke core, B-cells were ablated 5 days after dMCAO (Doyle et al., 2015). This prevented the delayed-cognitive deficits at 7 weeks after dMCAO (Doyle et al., 2015).

### **Neuroinflammation in obesity and stroke outcomes**

As previously mentioned, the inflammatory response is intimately involved in the progression of brain tissue damage in stroke, stroke outcomes, and obesity-related pathologies, which makes the link between obesity and stroke even stronger. Many studies have looked at the outcome of stroke in animal and human studies, while many others have attempted to understand the mechanisms mediating the relationship between obesity and stroke. There are different animal models used to study obesity, with some of

the most common ones being leptin-deficient (*ob/ob*) rodents, leptin receptor-deficient (*db/db*) rodents, or HFD-fed rodents (Haley & Lawrence, 2016).

In most animal studies, obesity generally leads to worse brain damage and behavioral outcomes after stroke (Haley & Lawrence, 2016). Studies that use HFD-fed rodents and *ob/ob* rodents found that obese animals tend to have larger infarcts after experimental ischemic stroke compared to normal diet animals or genetically normal animals (Cao, Du, Zhang, Yan, & Hu, 2015; Haley et al., 2017; E. Kim, Tolhurst, & Cho, 2014; Maysami et al., 2015; Terao et al., 2008).

Studies have also suggested that the duration of HFD and the duration of occlusion of blood flow in ischemic stroke models can impact the severity of tissue damage in the brain. For example, a study by Maysami et al. (2015) found that mice on either 2 or 3 months of HFD that underwent 30 minutes of tMCAO and 24 hours of reperfusion have no difference in infarct size compared to those mice on a normal diet, but mice that underwent 4 months of HFD and 30 minutes of tMCAO and 24 hours of reperfusion have a significantly larger infarct size compared those on normal diet (Maysami et al., 2015). In addition to length of consumption of HFD, longer periods of arterial occlusion during tMCAO increases the infarct size in HFD animals (Maysami et al., 2015). Mice on 6 months of HFD that underwent 20 minutes of tMCAO and 24 hours of reperfusion have no difference in infarct size compared to those in normal animals, but animals on 6 months HFD that underwent 30 minutes of tMCAO and 24 hours of reperfusion have a significantly larger infarct size compared to those normal animals (Maysami et al., 2015). However, not all studies agree that only longer periods of HFD

causes increased infarct areas. For example, a study done by Haley et al. (2017) found that 24 hours after tMCAO in mice on 3 days of HFD there was a 48% increase in infarct volume, although there is no difference in inflammatory markers in the periphery or brain (Haley et al., 2017). This suggests that even acute HFD consumption may cause significant increases in infarct size.

Many studies have found increased levels of pro-inflammatory chemokines and cytokines after ischemic stroke in obese animals compared to those levels in normal diet mice. These studies found that increased TNF, IL-6, chemokine C-C motif ligand-3 (CCL-3), chemokine C-X-C motif ligand (CXCL) and MCP-1 in obese animals, which exacerbates the neuroinflammatory response after ischemic stroke (Cao et al., 2015; Maysami et al., 2015; Terao et al., 2008). Maysami et al. (2015) showed an increase in neutrophil, microglia, and macrophage counts in the striatum 24 hours after 30 minutes of tMCAO in animals on 6 months of HFD compared those counts found in normal diet animals (Maysami et al., 2015). In addition, Teraro et al. (2008) found that leptin-deficient mice have increased white blood cell and platelet adhesion onto cerebral venules 4 hours after tMCAO compared to genetically normal mice (Terao et al., 2008) while another study by Cao et al. (2015) showed an upregulation of adhesion molecules VCAM-1 and ICAM-1 in the brain, which help leukocytes infiltrate into the injured neural tissue (Cao et al., 2015). Both these studies demonstrate an increased recruitment of immune cells to the brain in obese animals after ischemic stroke.

The BBB opening that occurs after stroke is also exacerbated in obese animals. Maysami et al. (2015) found a larger disruption of the BBB in the cortex at 24 hours after

30 min tMCAO in animals on 6 months of HFD compared to those on normal diet (Maysami et al., 2015). Teraro et al. (2008) also showed an increased opening on the BBB in leptin-deficient mice at 24 hours after tMCAO compared to that found in wild type mice (Terao et al., 2008). Studies suggest that increased disruption of the BBB is associated with increased level of MMPs in obese animals after ischemic injury. Db/db mice exhibit an increased degradation of occludin and collagen IV by MMP-9, which are components of the BBB, causing these mice to have increased BBB permeability after ischemic injury (Kumari, Willing, Patel, Baskerville, & Simpson, 2011). Another study by Deng et al. (2014) also showed increased BBB damage as well as increased hemorrhagic transformation in HFD animals after tMCAO (Deng, Zhang, Feng, Xiong, & Zuo, 2014). MMP-9 deficient mice on HFD have smaller hemorrhagic volumes in the brain after tMCAO compared to those found in genetically regular mice on HFD, and when placed on HFD they do not have worse functional motor outcomes compared to MMP-9 deficient mice on normal diet (Deng et al., 2014). These results indicate that MMP-9 is crucial contributor to the worsened stroke outcomes in obese animals.

Motor function after ischemic stroke tends to be worse in studies on obese animals (Deng et al., 2014; Dhungana et al., 2013). In a recent study done in our laboratory, motor functioning performance was examined at 1, 3, 7, 14 and 28 days after photothrombotic stroke in mice on HFD or normal diet. The photothrombotic stroke model was utilized in this study because of its ability to induce a thrombus at a specific area in the cortex. Since we were specifically studying motor functioning after stroke, we placed the stroke in the motor cortex. Consistent with the spontaneous motor recovery

found in the literature, animals in both diet group performed better in the motor function tasks during each successive time point. However, the animals on HFD have worse performance at all these time points compared to animals on normal diet.

Besides impaired motor functioning, obese human patients tend to have larger cognitive deficits after ischemic stroke compared to patients of normal weight (P. Li et al., 2016; Lu, Ren, Zhang, & Sun, 2016; Yong Zhang et al., 2012). In fact, it has even shown that normal weight human participants tend to perform better on certain cognitive tasks even after controlling for obesity-related diseases, such as stroke and diabetes (Nilsson & Nilsson, 2009). Currently, a few animal studies have looked at the association between post-stroke dementia and obese/diabetic rat models. Indeed, these studies indicate that obese/diabetic rats have increased cognitive deficits after ischemic stroke compared to normal rats that also underwent ischemic stroke, and these studies attributed this cognitive deficit to abnormal phosphorylation of tau proteins and beta-amyloid generation in the hippocampus (T. Zhang et al., 2009; Ting Zhang, Pan, Sun, Sun, & Sun, 2010). No animal studies have looked directly at obesity-induced neuroinflammation and its effects on delayed-onset cognitive deficits after stroke.

One interesting phenomenon worthy of mention is the obesity paradox in the context of stroke outcomes. While most preclinical/animal studies demonstrate that obesity is associated with impaired stroke recovery, there are some clinical studies showing that patients with higher BMIs actually had improved functional recovery, lower rates of short-term mortality, and lower rates of reoccurring strokes (Haley & Lawrence, 2016). It is unclear whether these studies actually reflect a true biological phenomenon,

or if this phenomenon is due to the differences in methodology and sampling in these studies (Haley & Lawrence, 2016).

### **Summary and current study**

Both obesity and ischemic stroke stimulate an immune response. Metabolic malfunctions such as insulin insensitivity observed in obesity are largely attributed to the chronic pro-inflammatory baseline which is characterized by the upregulation of pro-inflammatory mediators and immune cells like Th1 CD4+ cells, CD8+ cytotoxic cells, B-cells, and macrophages. On the other hand, the immune response after ischemic stroke in different studies are shown to be both beneficial and detrimental. The neuroinflammatory response at different time periods after ischemic stroke may have differential effects on stroke outcomes, but this is not well understood. It is also important to note that studies use many different models of experimental stroke, leading to the possibility that the neuroinflammatory phenotype and stroke outcomes may also depend on the stroke model used.

As mentioned earlier, most animal studies find that obesity exacerbates the neuroinflammatory response after stroke, leading to worse functional recovery. To further support this notion, our laboratory has shown that mice on HFD have significantly increased infarct size 72 hours after dMCAO compared to that normal diet animals 72 hours after dMCAO. This study also shows that HFD animals have higher levels of astrogliosis and microgliosis in the peri-infarct region 72 hours post-dMCAO, suggesting that the neuroinflammatory response may be contributing to the increased infarct size at

this time point. As previously indicated, it is found that HFD animals have worse motor recovery compared to normal diet animals after stroke. We additionally found that HFD animals have larger increases in pro-inflammatory mediators including NF- $\kappa$ B, NLRP3, MCP-1 and TNF 72 hours post-dMCAO. This supports previous literature that described upregulation of inflammatory pathways in the acute phase after stroke, including the inflammasome, in obese animal models.

While many studies, including our previous study, have characterized the neuroinflammatory response in obesity and its effects on stroke outcomes in the acute phase after ischemic, very few studies have considered this response in obese animal models during the chronic phase and its impact on functional recovery. In fact, no studies have looked directly at the effects of obesity-induced neuroinflammation on ischemic brain damage and cognitive functioning during the chronic phase.

Therefore, we were interested in characterizing the neuroinflammatory response and ischemic tissue damage in the chronic phase after stroke in obese animals. Furthermore, we would like to study whether these have an association with performance in cognition tasks. The study by Doyle et al. (2015) showed that mice have an increased adaptive immune response in the infarct core 7 weeks after stroke and that this likely contributes to the development of the cognitive deficits seen 7 weeks after stroke (Doyle et al., 2015). Based on the works of Doyle et al. (2015), our finding of a larger neuroinflammatory response and increased infarct expansion in obese animals, and the evidence of worse stroke outcomes in obese animals, we hypothesized that obese animals would have worse cognitive outcomes in the chronic phase after stroke compared to

normal diet animals. We also predicted that the neuroinflammatory response, e.g. astrogliosis, microgliosis, and increased T and B-cell infiltration, would be elevated in these obese animals during the chronic phase after stroke and contribute to increased brain tissue damage and ultimately delayed-cognitive deficits.

## **METHODS**

### **Animal usage**

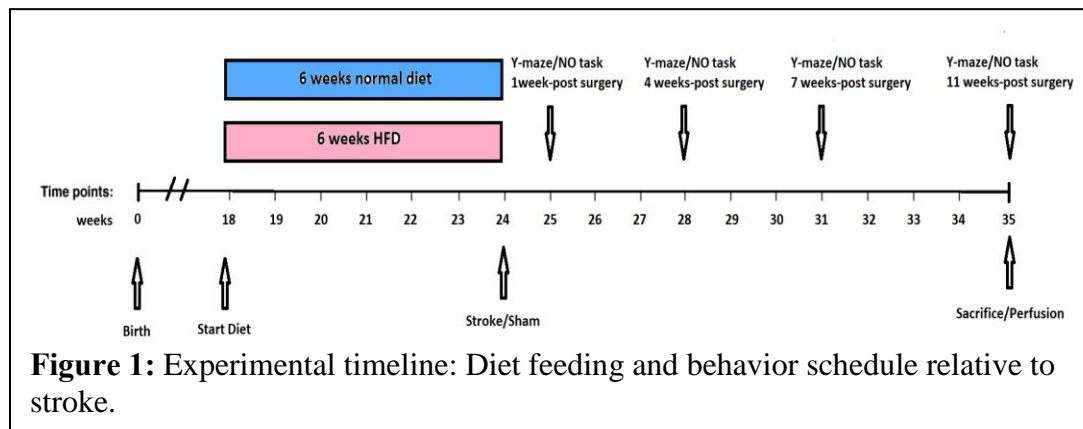
All use of animals was conducted according to protocols approved by the Stanford Institutional Animal Care and Use Committee and the NIH Guide for Care and Use of Animals. Forty 3-4-month-old female C57BL/6J mice (#664, The Jackson Laboratories, Bar Harbor, ME), were used in total for this study. Animals were given free access to food and water and kept on a 12-hour light/dark cycle. Each cage housed five mice.

### **High-fat diet and regular diet**

All HFD-fed animals were fed a HFD chow of 60% kCal fat (#D12492, Research Diets Inc., New Brunswick, NJ) for 6 weeks before surgery, while all the normal diet animals were fed a regular diet of 6% kCal fat (#2018SX, Harlan Laboratories, Indianapolis, IN) also for 6 weeks before surgery (Figure 1). After surgery, animals previously on HFD remained on HFD afterwards. Animals that received normal diet for 6 weeks remained on the normal diet afterwards.

## Stroke surgery

All mice used in our experiments underwent either a dMCAO to mimic an ischemic stroke or a sham surgery. For all surgeries, animals were placed in a chamber where anesthesia was induced (2% Isoflurane in 2 L/min 100% oxygen for 5 to 10 minutes) until no pedal reflex (movement from painful stimuli to foot) was observed in



each animal. Animals continued to remain on anesthesia throughout the surgery. All animals were maintained at rectal temperature of 37° C during surgery and recovery using a feedback heating blanket. During the dMCAO procedure, an incision was made along the animal's skull, through the skin, underlying connective tissue, and the temporalis muscle. Once the MCA was located, a craniotomy was drilled, exposing the dura right above the MCA. The dura was then punctured with a syringe and scrapped away, exposing the MCA, which was then cauterized. During sham surgery, the MCA was not cauterized once exposed, and otherwise the procedure is identical. The muscle and the skin was then folded back and the skin is sutured back together and mice are then injected with 25 mg/kg cefazolin (VWR #89149-888) and 1 mg/kg buprenorphine SR

(Zoopharm, Windsor, CO). The mouse was then placed under a heat lamp and monitored until it awoke. There are published studies that further describe the details of the dMCAO procedure (Doyle & Buckwalter, 2014; Doyle, Fathali, Siddiqui, & Buckwalter, 2012; Tamura, Graham, McCulloch, & Teasdale, 1981).

### **Experimental design**

Our study was a 2 x 2 design (dMCAO vs sham, HFD vs normal diet). In the text below, animals fed 6 weeks HFD that underwent dMCAO are called “dMCAO-HFD.” Animals fed 6 weeks normal diet that underwent dMCAO are called “dMCAO-normal diet.” Animals fed 6 weeks HFD that underwent sham surgery are called “Sham-HFD.” Animals fed 6 weeks normal diet that underwent sham surgery are called “Sham-normal diet.” Animals were sacrificed following behavioral assessment, 11 weeks after dMCAO or sham surgery.

### **Immunohistochemistry**

After sacrificing, animals were perfused with 0.9% NaCl containing 10 U/mL Heparin, and brains were dissected out and drop fixed in 4% paraformaldehyde in phosphate buffer for 24 hours prior to being moved to 30% sucrose in phosphate-buffered saline. 40 µm thick coronal brain sections were sectioned using a freezing sliding microtome (Microm HM430), collected sequentially in 12 tubes, and then stored in cryoprotectant medium (30% glycerin, 30% ethylene glycol, and 40% 0.5 M sodium phosphate buffer) at -20° C until further processed for immunohistochemistry. Standard

immunohistochemistry procedures were used to stain free floating sections. Sections were blocked with 3% donkey (Millipore, #S30-100mL), goat (Vector, #S-1000), or rabbit (Vector, #S-5000) serum for one hour. The brain sections were then incubated at 4°C overnight in primary antibody: anti-GFAP (rabbit, 1: 10,000, Dako, #Z 0334), biotinylated anti-NeuN (mouse, 1:500, Millipore, #MAB377B), or anti-CD68 (rat, 1: 1,000, Serotec, #MCA1957S). The following day, the brain sections were incubated for one hour in secondary antibody (1:500): anti-rabbit (goat, Vector, #BA-1000), or anti-rat (rabbit, Vector, #BA-4001), followed by ABC kit (Vector, #PK-6100) and 3,3'-Diaminobenzidine tetrahydrochloride (Sigma, #D5905). Sections that were stained for NeuN were then further counterstained for cresyl violet. For cresyl violet counterstaining, mounted sections were dehydrated, submerged in cresyl violet, and rehydrated. All tissue sections were mounted on glass slides and cover slipped with entellan.

### **Stroke size**

To assess stroke size, we took three different measurements for each animal: infarct area as a percent of contralateral hemisphere, ipsilateral hemisphere area as a percent of contralateral hemisphere area, and ipsilateral cortex area as a percent of contralateral cortex area. We immunostained 40 µm thick coronal sections spaced 240 µm apart with NeuN and counterstained with cresyl violet to visualize the infarction. Sections started anterior to and finished posterior to the stroke core. We then imaged the sections with a PathScan Enabler IV (Meyer Instruments, Houston, TX). For all three

measurements, ImageJ software (version 1.51c, 2017) was used to trace and quantify the desired area on each section.

To analyze infarct size and to control for the edema of the ipsilateral hemisphere that is frequently observed after stroke, we calculated the infarct area as a percent of contralateral hemisphere ( $(\text{infarct area}/\text{contralateral hemisphere area}) \times 100\%$ ). A researcher blinded to experimental groups of mice identified the five consecutive sections that most typically contained the infarcts seen in all the stroke animals. The infarct area as a percent of the contralateral hemisphere area for these five corresponding sections for all animal were calculated and then averaged together to get one average value per animal.

To analyze the degree of ipsilateral atrophy, we calculated the ipsilateral hemisphere area as a percent of contralateral hemisphere area ( $(\text{ipsilateral hemisphere area}/\text{contralateral hemisphere area}) \times 100\%$ ). This allowed us to compare the degree of atrophy in the ipsilateral hemisphere to the contralateral hemisphere. We measured the ipsilateral percent of contralateral for 12 sections per animal, spaced 480  $\mu\text{m}$  apart. We then took the average of the 12 sections per animal to get one average value for each animal.

To analyze the degree of ipsilateral cortical atrophy, we calculated the ipsilateral cortex area as a percent of contralateral cortex area ( $(\text{ipsilateral cortex area}/\text{contralateral cortex area}) \times 100\%$ ). This allowed us to analyze the degree of atrophy specifically in the ipsilateral cortex relative to the contralateral cortex. Due to time constraints, we took the measurements for the six middle sections of the 12 sections measured in the previous two

methods per animal. The six sections were spaced 480  $\mu\text{m}$  apart. We then took the average of the six sections per animal to get one average value for each animal.

### **Imaging analysis**

To image for reactive microgliosis/infiltrating MDMs and reactive astrogliosis, we immunostained three sections spaced 480  $\mu\text{m}$  apart for CD68 and GFAP, respectively. The stained sections were imaged at 20x (Keyence Microscope BZ-X710, BZ-X viewer, Osaka, Japan). Two images were captured in the peri-infarct cortex for each of the three sections per animal, one medial to and one lateral to the stroke core. Each image was taken in the cortex one view field distance (543  $\mu\text{m}$ ) away from the stroke border. For sham animals, we took images of where we would expect to find the peri-infarct cortex if these animals had undergone stroke. We quantitatively assessed the area covered by staining in an unbiased and blinded fashion. In ImageJ, images were set to an 8-bit color (black and white), and quantified at a less inclusive threshold and a more inclusive threshold. The less inclusive threshold encompassed only the soma while the more inclusive threshold included both the soma and processes. We then took the average of the three medial peri-infarct images for every animal to calculate the average relative percent area covered by GFAP in the medial peri-infarct area for each animal. We also did the same for the lateral peri-infarct images. Finally, we took the average of the relative percent area covered by GFAP in the medial peri-infarct area and the latera peri-infarct area per animal. This gave us an overall relative percent area covered by GFAP per animal. These values from animals in the same group were then averaged together to

get an overall relative percent area covered by GFAP for each group. The same steps were done for both the less inclusive images and the more inclusive images.

## Behavioral tasks

### Y-maze task

The Y-maze task is a spontaneous alternation behavior task and has been used in a variety of studies to measure hippocampal-dependent spatial memory in mice (Conrad, Galea, Kuroda, & McEwen, 1996; Fu et al., 2017; Reisel et al., 2002). Since this task requires mice to remember previous events, it is possible that this task may also involve other aspects of memory such as recognition. This task allows each mouse to freely explore a maze that consists of three arms, labeled A, B, and C (Figure 2). Mice tend to

explore a novel arm rather than the previous two arms that they explored (Stanford Medicine, 2017). For example, if a mouse went into arm A and arm B for its two previous choices, it would have preference to next go into arm C, since it had

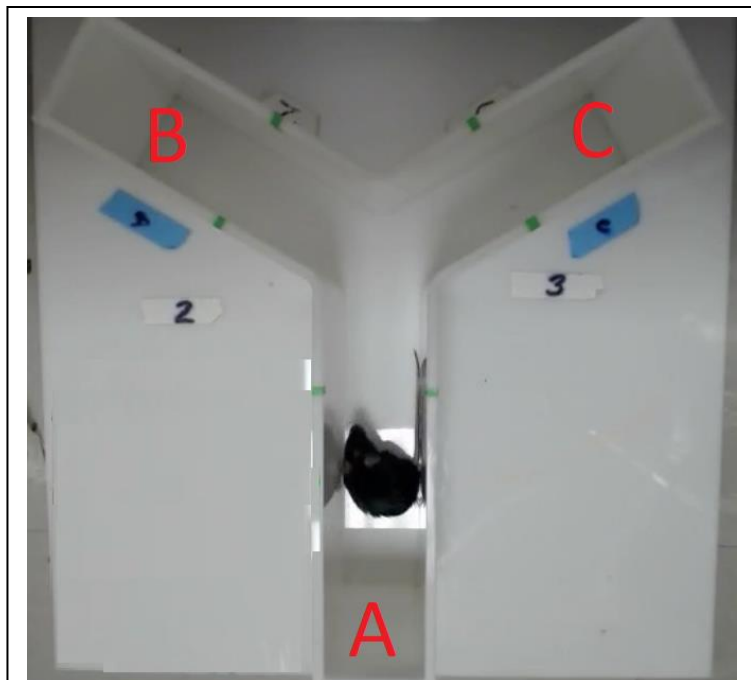


**Figure 2:** Schematic of Y-maze paradigm. Three arms labeled A, B and C.

not explored it in the previous two choices. We defined “alternation” as when the mouse enters an arm that is different from the last two choices. One hour before testing, the mice were moved to the testing room to allow them to acclimate to the environment. Each mouse was put into the Y-maze and given 5 minutes to freely explore. The 5-minute task was video recorded. The maze was cleaned with 70% ethanol between each mouse to prevent olfactory cues from affecting the behavior of the animals. A blinded researcher scored each 5-minute video, recording which arms and which order each mouse entered. The percent alternation was calculated as the proportion of choices differing from the previous two choices ( $\frac{\# \text{ of choices differing from the previous two}}{\text{total \# of alternation opportunities}}$ ). The total # of alternation opportunities is calculated as the total entries minus two. Each mouse was tested on the Y-maze 1 day prior to surgery, 1, 4, 7, and 11 weeks after surgery.

### **Novel object task**

The novel object task is a task used to test recognition memory (Leger et al., 2013), which includes the ability to recall previously explored objects, in mice. This task relies on the innate preference of mice to explore novel objects (NO) instead of objects they have explored before (Leger et al., 2013). Using this task, we can assess the memory of each mouse by looking at how much they explore the NO compared to a former object (FO). In phase 1 of this task, each mouse was put into an arena with two different but similar objects placed in the center of the arena with equal distances from the walls (Figure 3). Each mouse was given 5 minutes to freely explore the arena and the objects before being put back into its cage. For phase 2 of the task, one of the two objects in the

arena is replaced with a new object that is also different but similar to the object that is left in the arena (Figure 3).

Three to four hours after phase 1, each mouse was put into the arena again and allowed to explore freely for 5 minutes before being put back in its cage. The arena and object were wiped down with 70% ethanol between each trial to prevent olfactory cues from affecting the behavior of each mouse.

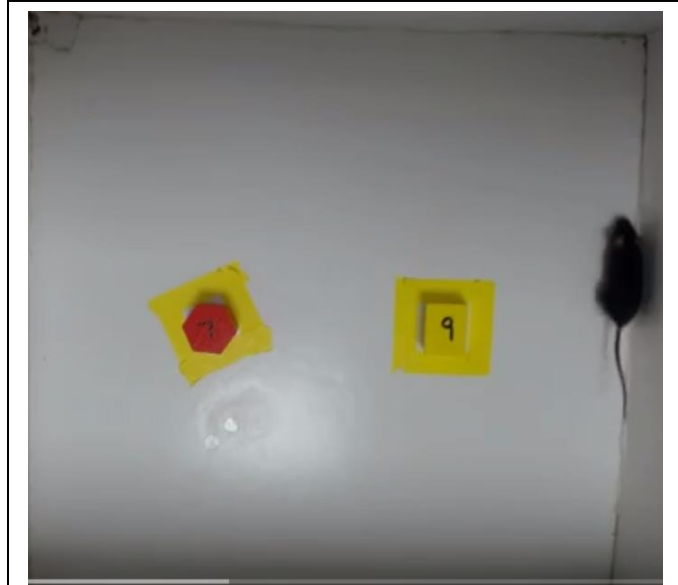


**Figure 3:** Schematic of Novel Object Task paradigm. NO arena consists of two different but similar objects. Any area inside the zone outlined by the yellow tape is 2 cm or less from the object.

Each 5-minute trial was video recorded and a blinded researcher watched each video and recorded the amount of exploration done by each mouse. We defined “exploration” of the objects in two ways: the number of times the mouse entered within 2 cm of the object and the total amount of time the mouse spent within 2 cm of the object. We refer to the space within 2 cm of the object the “exploratory zone”. Object recognition was quantified using a discrimination index (DI), defined as  $100 \times [(NO \text{ Time} - FO \text{ Time}) / (NO \text{ Time} + FO \text{ Time})]$ . Each mouse was tested on the NO task 1 day prior to surgery (baseline), and 1, 4, 7, 11 weeks after surgery.

## **Statistical analysis**

All values are shown as means  $\pm$  standard error of the mean (SEM). When only two groups were compared, a Student's *t*-test was used. When multiple groups were compared, we used an ordinary one-way analysis of variance (ANOVA) or two-way ANOVA and a Tukey's multiple group comparisons test, Sidak's multiple group comparisons test, or Dunnett's multiple group comparisons test as appropriate for post-hoc analysis. Data analysis was performed with GraphPad Prism 7 software. Parametric tests were chosen as we assumed all our datasets followed a normal distribution. We also utilized the Grubb's outlier test to identify any outliers within our dataset. We did not exclude any outliers from the analysis of our data set. Lastly, we performed multiple regression analysis to assess the effect of two independent variables on different dependent variables. All animals were randomized, concealed, and blinded to the experimenters. Samples that were defective due to tissue processing were also excluded from our analysis.

## **RESULTS**

### **HFD-fed animals experience weight gain while normal diet-fed animals maintain constant weight**

From multiple preliminary studies, we know that animals fed HFD consistently gain more weight than animals fed normal diet. In a previous study, we kept mice on either a HFD or normal diet for 6 weeks. Overall, a repeated measures two-way ANOVA

showed a significant difference in percent of original body weight between the two diet groups ( $p < 0.0001$ ). A Sidak's multiple comparisons post-hoc test suggested a significant difference in percent original body weight gain at 1,2, 4, 5, and 6 weeks between the

HFD group and normal diet

group (week 1,  $p < 0.001$ ;

week 2, 4, 5, 6,  $p < 0.0001$ ;

Figure 4). Six weeks of

HFD caused 36.7%

increase in weight while 6

weeks of normal diet

caused only 5.5% weight

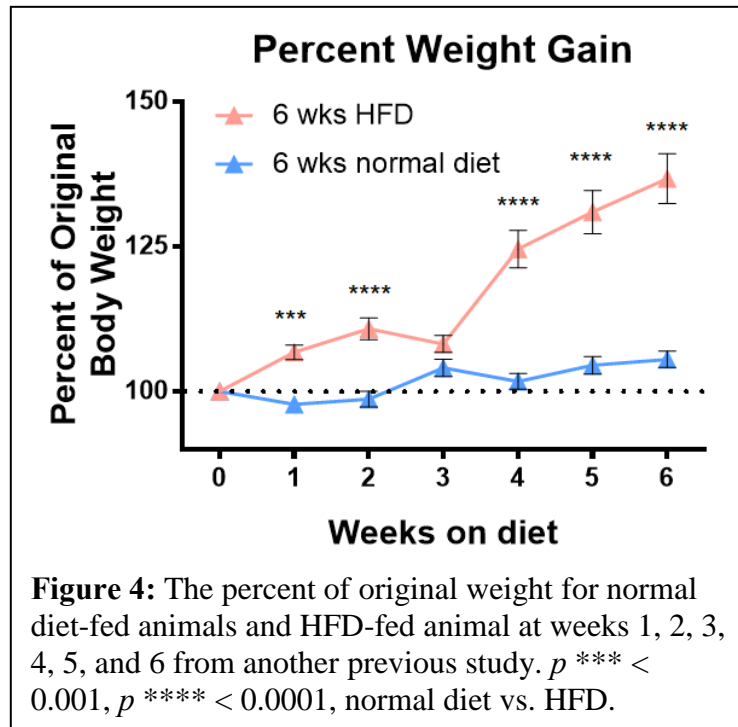
gain, which is a normal low

level of weight gain for this

normal diet (The Jackson

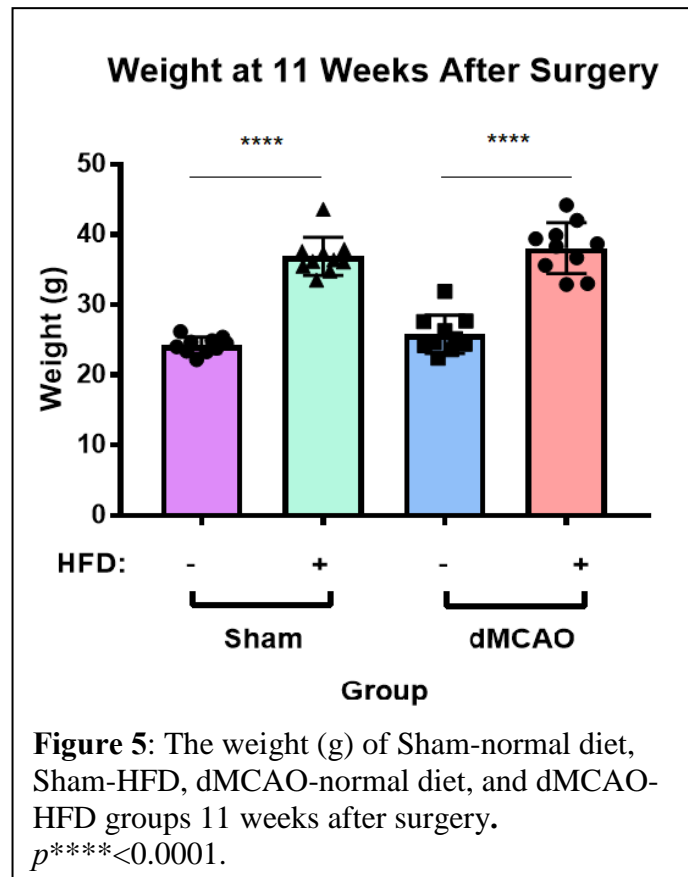
Laboratory, 2018). Therefore, we concluded that 6 weeks of HFD is sufficient to induce

significant weight gain.



Prior to sacrifice at 11 weeks after surgery, the weight of each animal was measured (Figure 5). Using a one-way ANOVA, we found significant differences in weight at 11 weeks after surgery between the four groups ( $p < 0.0001$ ). A Tukey's multiple comparison post-hoc test demonstrated that dMCAO-HFD animals weighed significantly more than dMCAO-normal diet animals ( $p < 0.0001$ ) while Sham-HFD

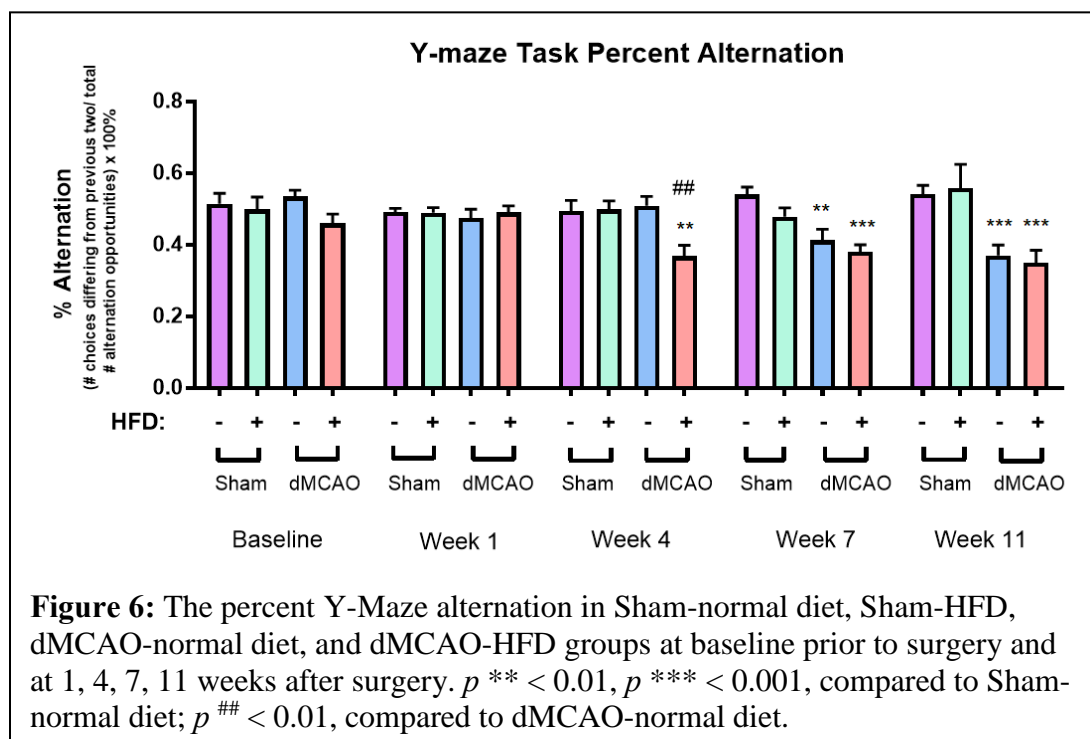
animals weighted significantly more than Sham-normal diet animals ( $p < 0.0001$ ). However, there was no difference in weight between dMCAO-HFD vs. Sham-HFD and dMCAO-normal diet vs. Sham-normal diet. In conclusion, we demonstrated that the type of diet but not the type of surgery had a significant effect on weight at 11 weeks after surgery.



### Following stroke HFD-fed animals have an earlier onset of cognitive deficit compared to normal diet-fed animals

To test our hypothesis that HFD-fed animals develop earlier and/or more severe cognitive deficits during the chronic period after stroke compared to normal diet-fed animals, we utilized the Y-maze task, a task used to assess memory in mice at 1, 4, 7, and 11 weeks after surgery. Overall, our results suggest that HFD-fed animals experience an

earlier onset of cognitive deficits after stroke. Using a two-way ANOVA, we found significant differences in percent alternation between the four groups ( $p < 0.0001$ ), but no difference in percent alternation between time points. Using a Dunnett's multiple comparisons post-hoc test (with Sham-normal diet animals as the control group), we found no significant difference in percent alternation between Sham-HFD and control

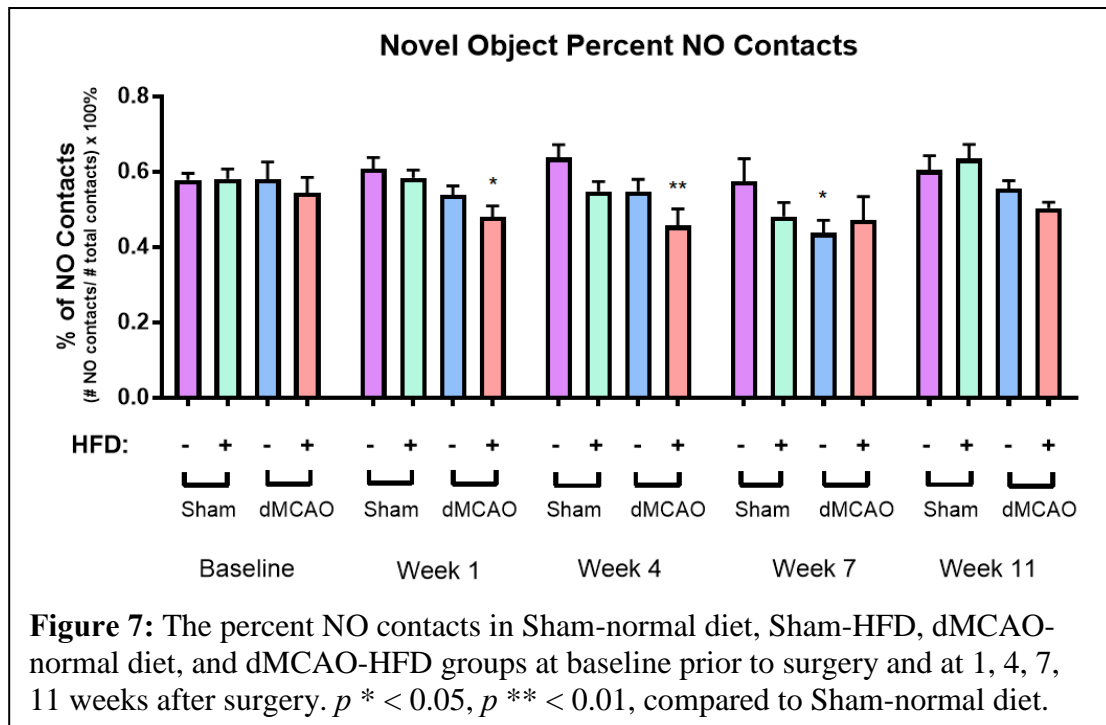


animals at all time points (Figure 6), suggesting that HFD alone does not significantly affect cognition at any of these time points. At 1 week after surgery, both the dMCAO-HFD and dMCAO-normal diet group did not perform differently from the control group, suggesting no deficits at 1 week after stroke in both diet groups. Interestingly, the dMCAO-HFD group did much worse at 4 weeks ( $p < 0.01$ ) while the dMCAO-normal diet group still did not perform much differently from the control group at this time point.

This excitingly suggests that HFD-fed animals but not normal-fed animal experienced memory deficits at just 4 weeks after stroke. As expected, both the dMCAO-normal diet and dMCAO-HFD group had worse deficits at 7 weeks compared to the control group (dMCAO-normal diet vs. control,  $p < 0.01$ ; dMCAO-HFD vs. control,  $p < 0.001$ ), which we continued to observe at 11 weeks (dMCAO-normal diet vs control,  $p < 0.001$ ; dMCAO-HFD vs control,  $p < 0.001$ ). A Tukey's multiple comparisons post hoc-test suggested that HFD-fed animals performed worse than dMCAO-normal diet animals at 4 weeks after surgery ( $p < 0.01$ ), but not at 1, 7, or 11 weeks after surgery. In conclusion, we demonstrated that HFD led to deficits in memory earlier after stroke (at 4 weeks instead of 7 weeks). Note that although HFD did not lead to more severe deficits at 7 weeks and beyond compared to normal diet, the Y-maze task has a floor effect—mice cannot do worse than random movement. Therefore, this experimental design only allows us to test the onset of deficits but not whether they are worse in one impaired group than another.

In addition to utilizing the Y-maze task, we also used the NO task to test memory after dMCAO in both diet groups at weeks 1, 4, 7, 11 after surgery. Overall, a two-way ANOVA suggested significant differences in percent NO contacts between the four groups ( $p < 0.0001$ ) and between time points ( $p < 0.05$ ). Using a Dunnett's multiple comparisons post-hoc test (with the Sham-normal diet group as the control), we found that Sham-HFD and control animals did not have a significant difference in percent of NO contacts at all time points, similar to what we found in the Y-maze task (Figure 7).

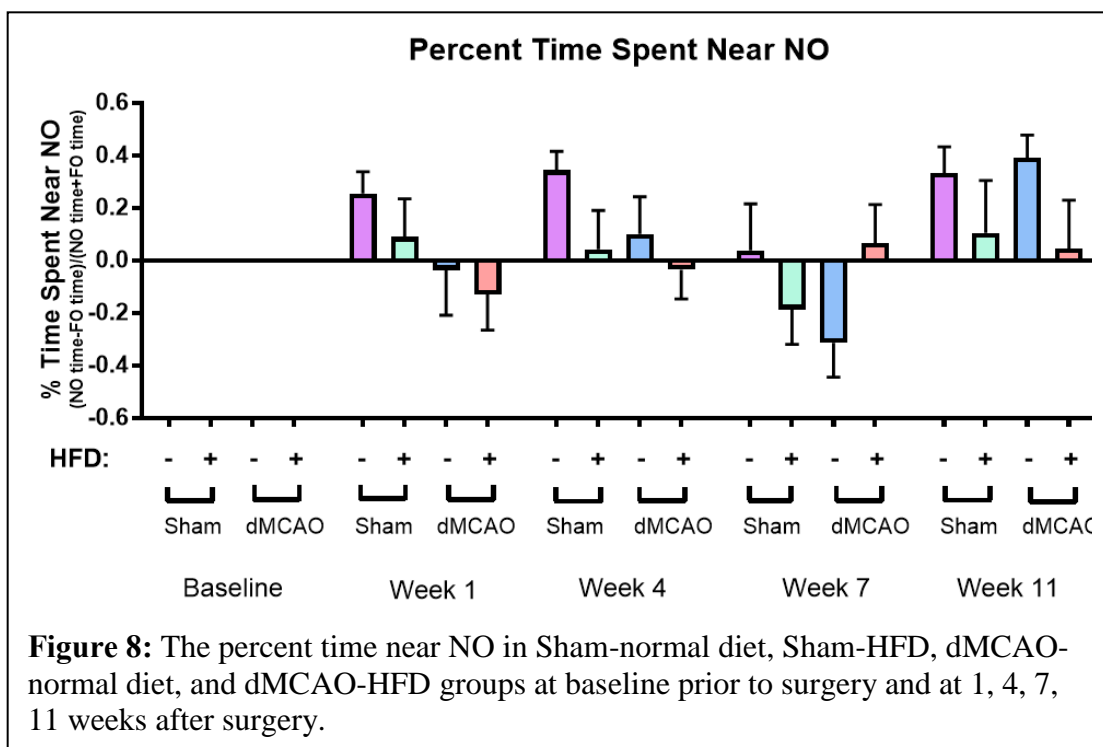
This suggests that recognition memory is also not affected by diet alone at these time points. Surprisingly, we observed worse performance in dMCAO-HFD animals compared to the control group at just 1 week after surgery ( $p < 0.05$ ), while dMCAO-



normal diet did not perform differently than the control group. The onset of deficits was seen much earlier using this task, whereas the deficits were seen later in the Y-maze task (at week 4). This deficit in the dMCAO-HFD group persisted at 4 weeks after stroke ( $p < 0.01$ ), whereas the dMCAO-normal diet group continued to perform similarly to the control group at this time point. Interestingly, we started to observe a deficit in dMCAO-normal diet animals ( $p < 0.05$ ) but not dMCAO-HFD animals at 7 weeks. Furthermore, both the dMCAO-normal diet and dMCAO-HFD animals performed similar compared to the control animals at 11 weeks. A Tukey's multiple comparisons post-hoc test showed no significant differences between dMCAO-HFD and dMCAO-normal diet animals at

any time points. In conclusion, we demonstrated that HFD caused earlier onset of deficits in cognition after stroke (at 1 and 4 weeks vs. 7 weeks). Both diet groups eventually experienced improved memory, at 7 weeks for dMCAO-HFD animals and 11 weeks for dMCAO-normal diet animals, suggesting that both diet groups experienced spontaneous recovery in the NO cognitive task.

Another method of measuring exploration in the NO task is to consider the total time spent at each object, which is the total time that each mouse spent within the



exploratory zones associated with each object. To analyze our dataset using the two-way ANOVA, we had to delete the data from the baseline time point for all groups, since we were missing all the data for the Sham-HFD and Control group. Using a two-way ANOVA after this exclusion, we found significant differences in percent time spent near

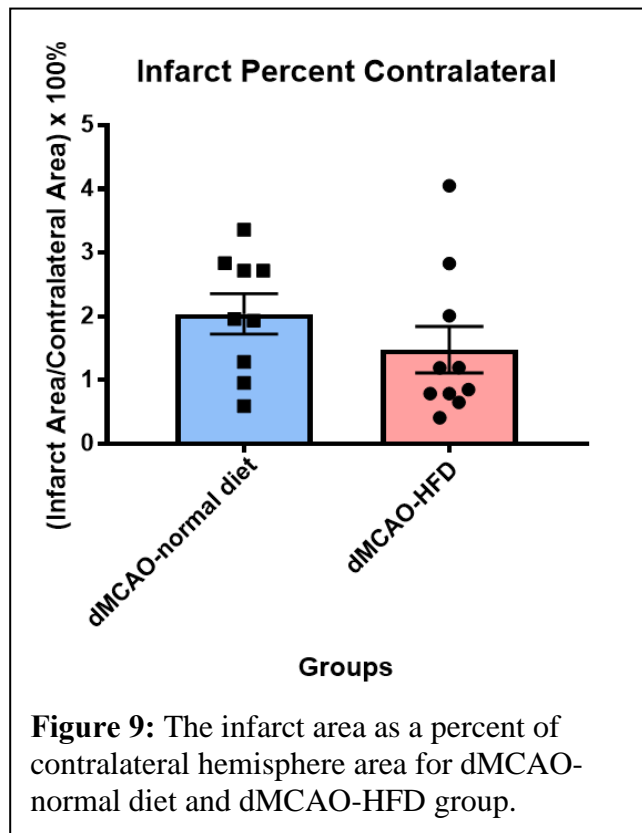
NO between the four groups ( $p < 0.05$ ) and between time points ( $p < 0.05$ ). A Dunnett's multiple comparisons post-hoc test (with Sham-normal diet animals as the control) suggested no significant differences between the different groups and the control group at every time point. Overall, the percent time near NO seemed to be variable and we did not see any expected patterns (Figure 8). In fact, we found negative values in the percent time spent near NO in different groups at various time points, which demonstrates that on average, these mice spent more time near the FO than near the NO.

### **Stroke size does not differ between dMCAO-HFD animals and dMCAO-normal diet animals 11 weeks after dMCAO**

To see whether this earlier onset of cognitive-deficits observed in the dMCAO-HFD animals was associated with increased ischemic brain tissue damage, we measured the infarct size, the degree of ipsilateral hemisphere atrophy, and degree of ipsilateral cortex atrophy at 11 weeks after stroke. As mentioned earlier, we calculated the average infarct area as a percent of contralateral hemisphere in five brain sections per animal to control for ipsilateral edema typically observed in our dMCAO stroke model. Using an unpaired  $t$ -test, we found no difference in the infarct as a percent of the contralateral hemisphere between the dMCAO-normal diet group and dMCAO-HFD group (Figure 9).

While performing the infarct area, we noticed that many of the tissue sections in most animal did not have obvious stroke cores and that most of the areas that were

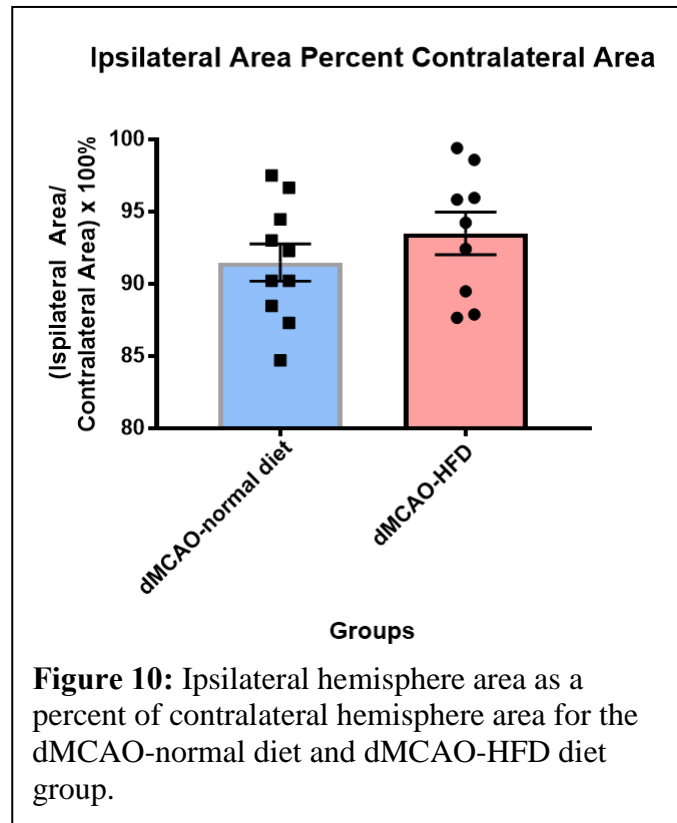
supposed to contain the stroke core were very small perhaps due to brain remodeling over the 11 weeks since stroke (Z. G. Zhang & Chopp, 2015). This made it difficult to accurately measure the infarct area in each of those sections. Furthermore, we qualitatively noticed that the tissue surrounding the infarct area tended to curve in, making it even more difficult to predict where the infarct area would be in those sections missing the stroke core.



Because of the difficulty of accurately measuring the infarct area with this method, we assessed brain tissue damage by measuring the remaining ipsilateral hemisphere area as a percent of the contralateral hemisphere area. This method seemed to produce less subjective results and allowed us to assess the degree of ipsilateral hemisphere atrophy, which is more ideal since we qualitatively noticed that the ipsilateral hemisphere tended to be smaller than the contralateral hemisphere. We excluded the areas of ventricles in our measurements since ventricular sizes are known to increase after stroke when there is brain atrophy. Using an unpaired *t*-test, we also found no

difference in the ipsilateral hemisphere area as a percent of contralateral hemisphere area between the dMCAO-normal diet group and dMCAO-HFD group (Figure 10).

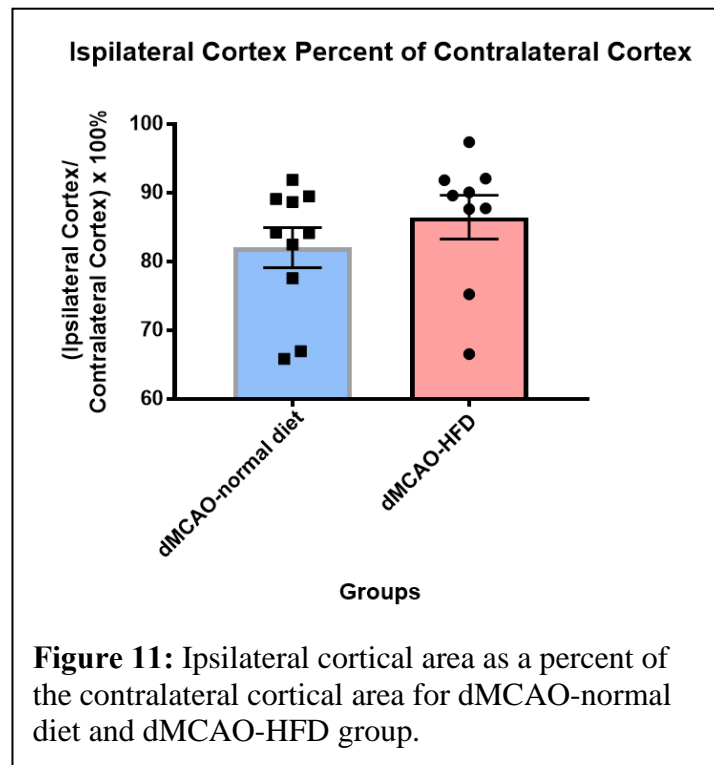
Since we did not find a difference by measuring the degree of atrophy in the entire ipsilateral hemisphere, we decided to focus our analysis on the cortical regions of the tissue sections. In the dMCAO stroke model, the infarct is in the cortex. Therefore, we decided that assessing the degree of ipsilateral cortical atrophy by



calculating the ipsilateral cortical area as a percent of contralateral cortical area would give us results that would more accurately reflect the amount of damage caused by dMCAO. An unpaired *t*-test suggested no difference in the ipsilateral cortical area as a percent of the contralateral cortical area between the dMCAO-normal diet group and the dMCAO-HFD group (Figure 11). In conclusion, we demonstrated that diet does not influence infarct size or the degree of ipsilateral tissue atrophy at 11 weeks after stroke.

## Diet does not dramatically affect the degree of astrogliosis 11 weeks after dMCAO

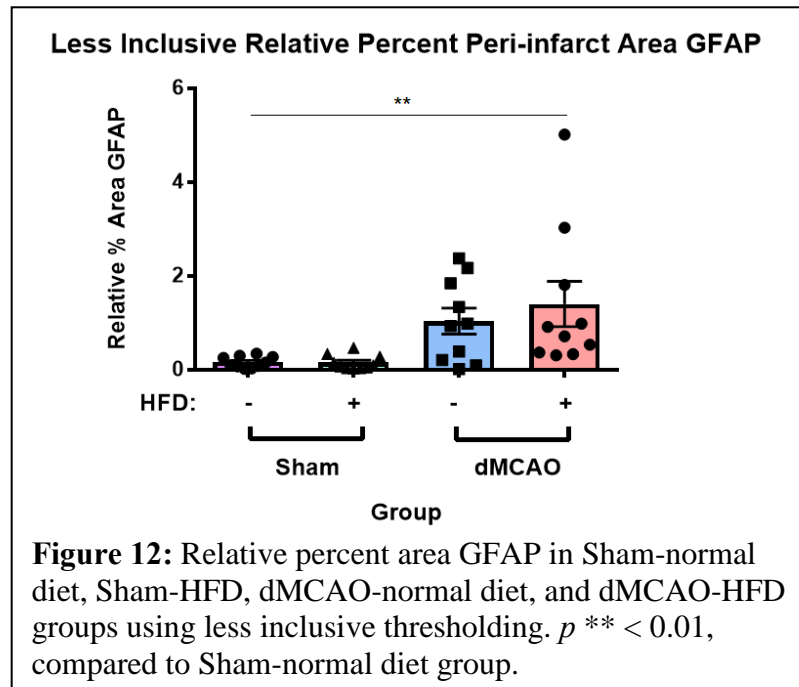
To characterize the neuroinflammatory response at 11 weeks after dMCAO or sham in animals on HFD or normal diet, we stained brain sections for GFAP and measured the percent of the peri-infarct area covered by this cell marker. GFAP is a surface



marker found in astrocytes that is dramatically upregulated after neural insult and is therefore an indicator of reactive astrogliosis (Fawcett & Asher, 1999). First, we applied a less inclusive threshold, which only included the most intense areas of GFAP reactivity, which is generally limited to cell bodies. Using a one-way ANOVA on our data obtained from less inclusive thresholding, we found significant differences in relative percent of the peri-infarct area covered by GFAP between the four groups ( $p < 0.01$ ). A Dunnett's multiple comparisons post-hoc test (using Sham-normal diet animals as the control) suggested that the relative percent peri-infarct area covered by GFAP in dMCAO-HFD is significantly higher than control ( $p < 0.01$ ), with the dMCAO-HFD group having an

8.47-fold larger percent area covered by GFAP (Figure 12). However, there were no significant differences in the percent area covered by GFAP between the dMCAO-normal

diet group and control. We also found no difference between the Sham-HFD and the control group. To test for differences in GFAP staining between all the groups, we used a Tukey's multiple

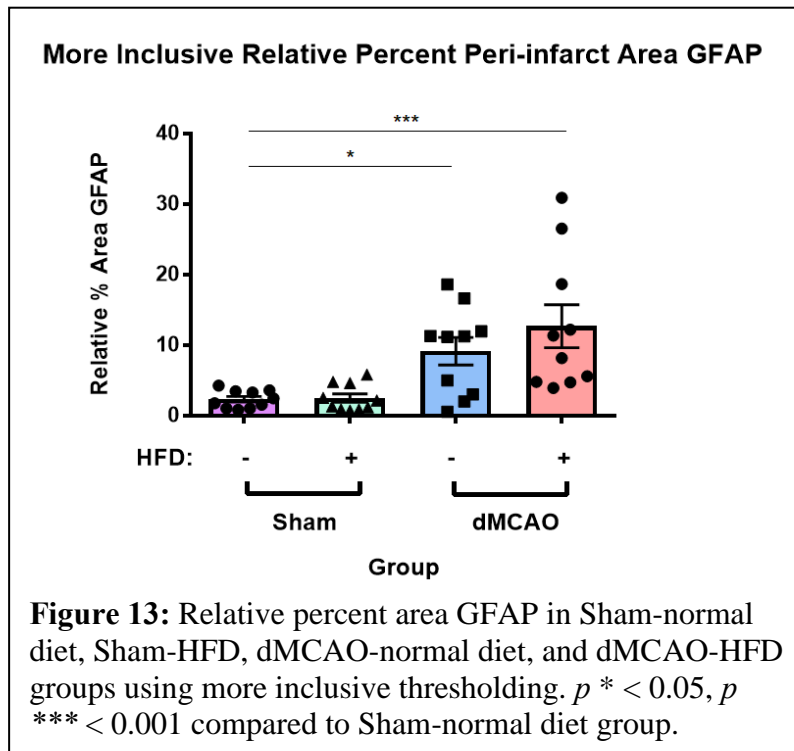


comparisons post-hoc test and found no differences in percent area covered by GFAP between the dMCAO-HFD and dMCAO-normal group. In conclusion, we demonstrated that HFD leads to increased coverage of the peri-infarct area by astrocytic cell bodies at 11 weeks after stroke. We also show that stroke or HFD alone does not lead to increased coverage of astrocytic cell bodies at this time point.

To see if there were differences in the morphology of astrocytes in the peri-infarct area between the four groups, we also utilized a more inclusive threshold, which includes both GFAP-positive cell bodies and processes. A one-way ANOVA suggested a significant difference in percent area covered by GFAP between the four groups ( $p <$

0.001). Using a Dunnett's multiple comparisons post-hoc test (with Sham-normal diet animals as the control), we discovered a significant increase in percent area covered by GFAP in both the dMCAO-HFD and dMCAO-normal diet group compared to the control group (dMCAO-normal diet vs control,  $p < 0.01$ ; dMCAO-HFD vs control,  $p < 0.001$ ; Figure 13). The percent area covered by GFAP in dMCAO-HFD animals was 5.4 folds

higher than the those found in control, while the percent area covered by GFAP in dMCAO-normal diet animals was 3.9 folds higher than those found in control. This is interesting, since we did not observe a



significant increase in percent area covered by GFAP in dMCAO-normal diet animals using a less inclusive threshold. Like our results from less inclusive thresholding, we found no difference between the Sham-HFD group and the control group. A Tukey's multiple comparisons post hoc-test revealed no differences in percent area covered by GFAP between the dMCAO-HFD and dMCAO-normal group. In conclusion, we demonstrated that astrocytes in the peri-infarct area adopt a more reactive phenotype at

11 weeks after stroke in both diet groups, and that HFD alone does not lead to a larger degree of reactive morphology in astrocytes.

### **Microglia/MDM activation is increased in HFD-dMCAO animals compared to dMCAO-normal diet animals 11 weeks after stroke**

To characterize the microglial response and degree of MDM infiltration at 11 weeks after dMCAO or sham, we stained tissue sections with CD68. CD68 is a surface marker known to be expressed on phagocytotic microglia and macrophages, and is an indicator of reactive microgliosis/infiltrating MDMs. To include just the cell bodies of microglia/MDMs in our analysis, we used a less inclusive thresholding. A one-way ANOVA showed significant differences in the relative percent area covered by CD68 between the four groups at 11 weeks after surgery ( $p < 0.01$ ). A Dunnett's multiple comparisons post-hoc test, comparing each group to the Sham-normal diet group (control), demonstrated a significantly larger relative percent area covered by CD68 in the dMCAO-HFD compared to the control group ( $p < 0.01$ ), as expected (Figure 14). There were no differences between the dMCAO-normal diet group and the control group. We also did not find any differences between Sham-HFD and control animals. Using a Tukey's multiple comparison post-hoc test, we found a significantly larger relative percent area covered by CD68 in the dMCAO-HFD group compared to the dMCAO-normal diet group ( $p < 0.05$ ). In conclusion, we demonstrated that HFD leads to increased coverage of the peri-infarct area by cell bodies from activated microglia/MDMs at 11

weeks after stroke. Furthermore, stroke or HFD alone does not lead to increased CD68-stained cell bodies at this time point, suggesting that stroke and HFD interact to produce increased microglia/MDM numbers in dMCAO-HFD mice at 11 weeks after stroke.

When we used a one-way ANOVA on our data obtained from more inclusive thresholding, we found significant differences in the relative percent of peri-infarct area covered by CD68 between the four groups at 11 weeks after surgery ( $p < 0.01$ ). Followed this up with a Dunnett's multiple comparisons post-hoc test (with the control group being the Sham- normal diet animals), we demonstrated a significant difference between the

relative percent area

covered by CD68

between the dMCAO-

HFD and control

animals ( $p < 0.01$ ;

Figure 15). We did not

find a difference

between dMCAO-

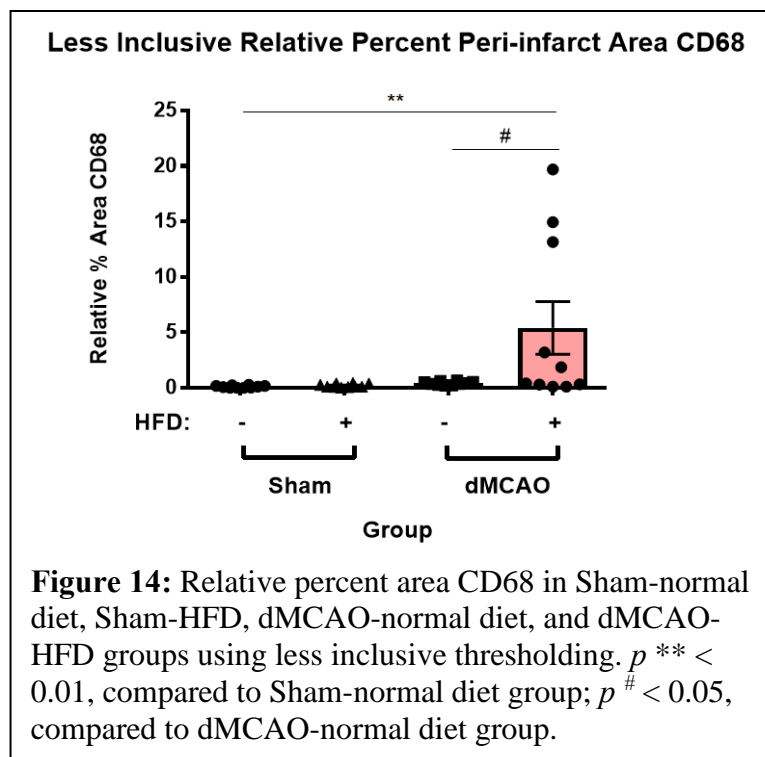
normal diet and control

animals nor between the

Sham-HFD and control

animals. A Tukey's multiple comparisons post-hoc test revealed significantly higher

relative percent covered by CD68 in the dMCAO-HFD group compared to the dMCAO-

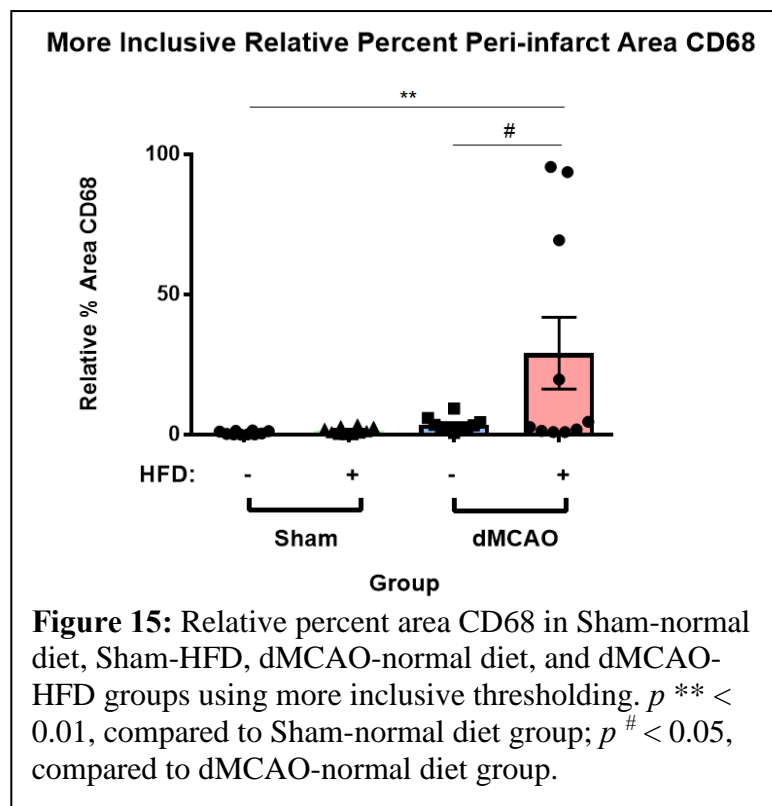


normal diet ( $p < 0.05$ ). These results suggest that HFD leads to a larger degree of reactive morphology in active microglia/MDMs in the peri-infarct area at 11 weeks after stroke. We also found that stroke or HFD alone does not lead to increased reactive phenotype at this time point.

### Body weight does not correlate with the degree of cortical atrophy at 11 weeks after stroke

We next asked if there was a relationship between weight at sacrifice and the degree of ischemic brain damage (Figure 16). Since we thought the ipsilateral cortex area as a percent of

contralateral cortex area most accurately reflected the tissue damage caused by dMCAO, we compared the data from this method to the weight of animals at sacrifice using multiple regression analysis.

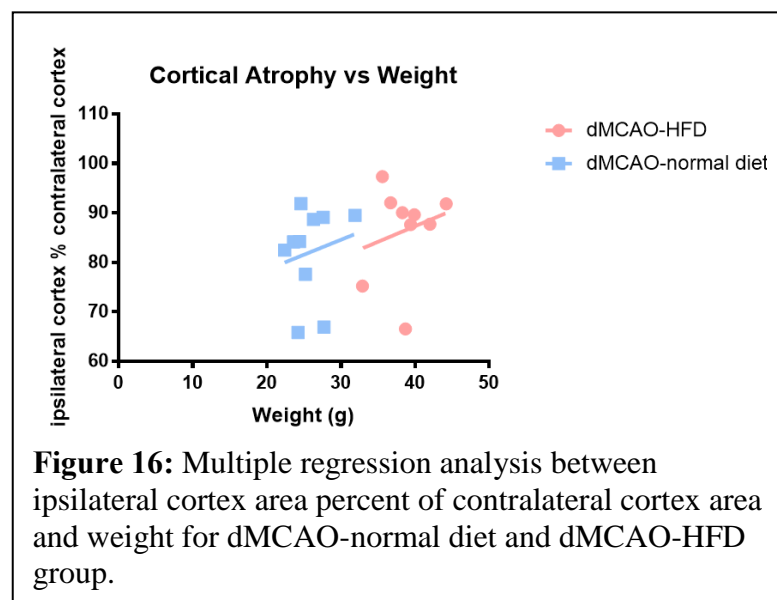


There was no relationship between mouse body weight and degree of cortical atrophy in

the dMCAO-HFD group. This was also the case for the normal diet group, indicating there is not a correlation between body weight and infarct size 11 weeks after dMCAO in either diet condition. Furthermore, we also found no relationship between weight and cortical atrophy after pooling the data together from dMCAO-HFD and dMCAO-normal diet groups, confirming no correlation between weight and cortical atrophy regardless of diet. From the small R squared values, we infer that the regression model only explains a small amount of the variability between weight and cortical atrophy in the dMCAO-HFD group, dMCAO-normal diet group, and the pooled group.

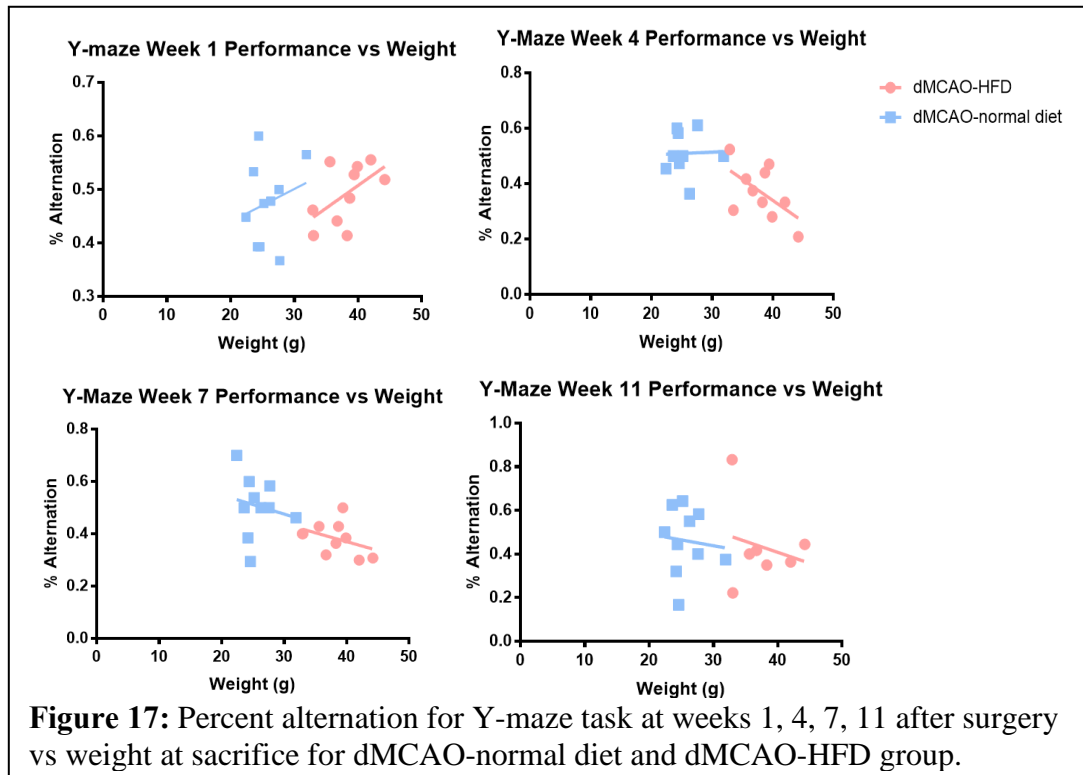
### Body weight is correlated with Y-maze performance at week 4 and 7 after stroke

To see whether diet affected the relationship between weight measurements taken at sacrifice and cognition at different time points, we also utilized a multiple regression analysis (Figure 17). At every time point after stroke at which cognitive performance was



measured, separate regression lines for both the dMCAO-HFD and dMCAO-normal diet

group did not have slopes significantly different from zero, indicating there was no correlation between weight and cognition in both diet groups at all time points after



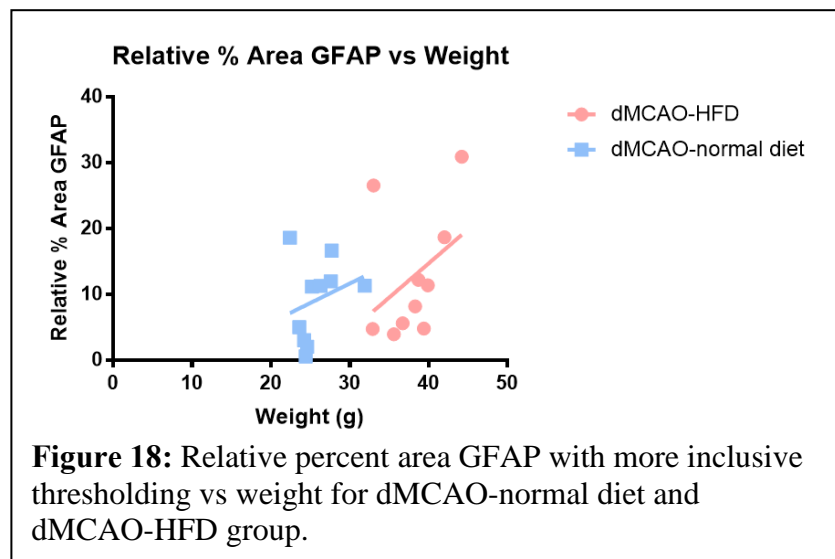
stroke. However, when we pooled the data together from the dMCAO-HFD and dMCAO-normal diet group for each time point, we found at 4 weeks after stroke, there was a significant negative relationship between weight and Y maze performance ( $R$  squared = 0.4858,  $p < 0.001$ ). This was also true at 7 weeks after stroke ( $R$  squared = 0.3676,  $p < 0.01$ ). Taken together, these results suggest that cognition at 4 and 7 weeks after stroke tend to decrease with increasing weight, regardless of diet. However, from the relatively small  $R$  squared values at the different time points, we also infer that the regression model only explains a relatively small amount of the variability between weight and cortical atrophy in the dMCAO-HFD group, dMCAO-normal diet group, and

the pooled group at different time points. At all time points, there were no significant difference between the slopes of the regression equations for the dMCAO-HFD and dMCAO-normal diet group, suggesting that the relationship between weight and performance on the Y maze did not depend on type of diet.

### Body weight is not correlated with the degree of astrogliosis 11 weeks after stroke

Next, we asked whether there was a relationship in either diet condition between

the degree of astrogliosis in the peri-infarct area and body weight at sacrifice (Figure 18). We utilized the relative percent peri-infarct area



covered by GFAP measured with a more inclusive threshold to compare with weight since more inclusive thresholding measured the area covered by both cell body and cell processes expressing GFAP, therefore being a better measure of reactive astrogliosis. Using a multiple regression analysis, we found no significant correlation between the degree of astrogliosis and body weight in both the dMCAO-HFD and the dMCAO-normal diet group, suggesting no correlation between body weight and the degree of

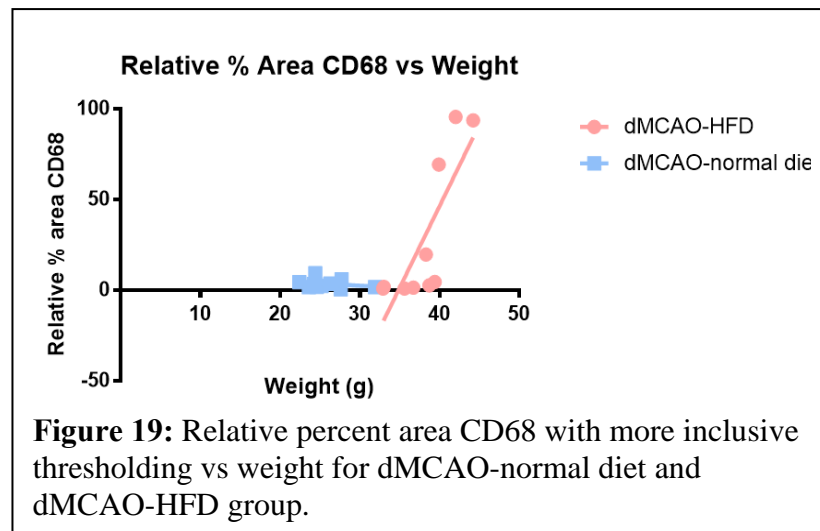
astrogliosis in both diet conditions at 11 weeks after stroke. After pooling the data from dMCAO-HFD and dMCAO- normal diet group together, we still did not find an association between body weight and the degree of astrogliosis, suggesting no correlation between these two variables regardless of the type of diet. The small R squared values found in the dMCAO-HFD group, dMCAO-normal diet group, and the pooled group demonstrated that the regression model can only explain a small amount of the variability between weight and degree of astrogliosis. Since there was no significant difference between the slopes of the regression lines for the dMCAO-HFD group and the dMCAO-normal diet group, we concluded that the correlation between weight and degree of astrogliosis at 11 weeks after stroke did not depend on the type of diet.

### **Body weight is not correlated with the degree of microgliosis/infiltrating MDMs 11 weeks after stroke**

Finally, to assess the effects of diet on the correlation between the degree of reactive microgliosis/infiltrating MDMs in the peri-infarct area and the weight at sacrifice, we also utilized a multiple regression analysis (Figure 19). Again, we used our results obtained from more inclusive thresholding to compare with weight. We found a significant positive correlation between body weight and degree of reactive microgliosis in the dMCAO-HFD group ( $R^2 = 0.6559$ ,  $p < 0.01$ ), suggesting that the degree of microgliosis increased with body weight at 11 weeks after stroke in animals on HFD. However, we did not see an association between weight and degree of microgliosis in the

dMCAO-normal diet group. Pooling the data together from dMCAO-HFD and dMCAO-normal diet group gave us a positive association between body weight and degree of microgliosis (R squared = 0.4069,  $p < 0.01$ ). This suggests that without considering the effects of diet, the degree of microgliosis increase with body weight. We also found a significant

difference between the slopes of the regression lines for the dMCAO-HFD group and the dMCAO-normal diet group ( $p <$



0.01), demonstrating that the relationship between weight and degree of microgliosis at 11 weeks after stroke depends on the type of diet.

### Outlier tests

To test for outliers in our datasets, we utilized the Grubb's test. We found one animal in the Sham-HFD group whose weight was an outlier when analyzing weight at 11 weeks after surgery. We did not find any outliers in our datasets used for the different methods of calculating ischemic brain tissue damage. We found one animal in the dMCAO-HFD group whose relative percent area GFAP was an outlier when analyzing

the relative percent of peri-infarct area covered by GFAP using less inclusive thresholding. We did not exclude any outliers since we were unsure if these data points were due to biological variability or experimental errors.

## DISCUSSION

Ischemic stroke is a neurological disease that has high morbidity rates and leads to the onset of cognitive deficits. Obesity is one of the risk factors for ischemic stroke, and it is thought that a larger neuroinflammatory response in obese patients can be the cause of worse stroke outcomes. In particular, stroke patients who are obese have worse cognitive deficits (P. Li et al., 2016; Lu et al., 2016; Yong Zhang et al., 2012) However, very little is known about the mechanisms, such as neuroinflammation, which determine the onset of cognitive deficits in obese patients, especially in the chronic phase after stroke. Therefore, we conducted a study to test whether obese mice had an earlier onset of delayed-cognitive deficits compared to normal weight mice, and whether this increased cognitive deficit was associated with larger strokes and increased neuroinflammatory response during the chronic phase. In summary, we found that HFD-fed animals had an earlier onset of cognitive deficits compared to normal diet-fed animals after stroke. We also found that both diet groups had persistent reactive astrogliosis in the chronic phase after stroke while reactive microgliosis was present only in the HFD-fed

animals during that time point, suggesting that HFD led to a larger persistence of neuroinflammation.

Consistent with the findings of Doyle et al. (2015), we demonstrated that normal diet-fed animals had significant deficits in memory at 7 weeks after stroke compared to Control animals, as suggested by the results from the Y-maze task. It is noteworthy that we observed similar deficits on the Y-maze task using our dMCAO stroke model, whereas the study by Doyle et al. (2015) utilized the distal middle cerebral artery occlusion with hypoxia (DH) stroke model, indicating this task is able to detect cognitive deficits in the chronic phase after stroke in multiple rodent models of ischemia. Memory deficits were also evident in HFD-fed mice at the 7-week time point, as expected. Interestingly, we saw the onset of memory deficits in HFD-fed animals at just 4 weeks after stroke, whereas normal diet-fed animals did not have this deficit at this time point. These findings suggest that HFD-fed animals tend to have an earlier onset of memory deficits compared to normal weight animals after stroke. At 11 weeks after stroke, we saw that mice in both diet conditions continued to perform worse significantly worse in the Y-maze compared to the non-stroke normal diet animals, suggesting that this delayed-cognitive deficit persists beyond the 7-week time point described in Doyle et al.'s (2015) study.

In addition, we demonstrated that heavier animals tend to have more severe cognitive deficits than lighter animals at 4 and 7 weeks after stroke. While we found that HFD-fed mice on average experienced cognitive deficits earlier after stroke at 4 weeks compared to normal-diet mice, the heavier mice in the dMCAO-HFD group did not

necessarily have a larger deficit compared to the other animals in that same group at that time point. This may suggest that once the animals reach a certain level of adiposity, a further increase in body weight does not worsen cognitive deficits even further. These results may also be due to a flooring effect in the behavioral task, where the performance in the Y-maze does not accurately reflect the degree of deficits once the animals perform worse than a certain level. Finally, it is important to note that all four groups had a percent alternation of around 50% at baseline and week 1 after surgery, suggesting that they were not performing above chance. Therefore, it makes it more difficult to interpret whether the significant decreases in percent alternation at later time points truly reflect worse performance.

Our findings from the novel object recognition memory task were largely consistent with our findings from the Y-maze task. Using the NO task, we found a significant deficit in normal diet-fed animals at 7 weeks after stroke compared to the Control animals. Interestingly we saw an even earlier deficit in HFD-fed animals at just 1 week after stroke, which may suggest that certain aspects of cognitive functioning, such as recognition memory, may be affected earlier by obesity than other aspects like spatial memory. While there is evidence that stroke can affect different aspects of cognitive functions, like executive functioning, memory, and learning (Al-Qazzaz, Ali, Ahmad, Islam, & Mohamad, 2014) there is no clear evidence directly supporting that decline in recognition memory in particular occurs earlier than the decline in spatial memory. As mentioned earlier, animals may also utilize other cognitive skills when performing in the Y-maze such as recognition memory, which is what the NO task supposedly measures.

This makes it uncertain whether our results suggest an earlier onset of deficit in one component of cognition compared to another. This deficit in recognition memory continued to be seen in HFD-fed animals at 4 weeks after stroke.

Surprisingly, performance of obese animals on the NO task had improved to control levels at 7 and 11 weeks after stroke, while normal diet-fed mice did not show improvements until 11 weeks. This may suggest that both normal weight and obese animals experienced a functional recovery in recognition memory during the chronic phase, and that obese animals experienced this recovery earlier than normal weight mice. This contradicts our findings from the Y-maze task, where we found an onset of cognitive deficits at 7 weeks in HFD-fed animals and continuation of this deficit at 11 weeks in both diet groups.

We hypothesize that the NO task may not be a reliable behavioral paradigm for testing recognition memory deficits in our dMCAO stroke model. Many different factors may confound the results such as any differences in the physiology and genetics of the animals or the environment of the animals and result in variability in these behavioral tasks (Nature Neuroscience, 2009; Sousa N., Almeida O. F. X., & Wotjak C. T., 2006). Examples of factors in the environment that can change animal behavior include the way the animals are handled by the investigator, the lighting during the behavioral tasks, and the time of the day the task was done (Sousa N. et al., 2006). Because of this, there is considerable natural variability in rodent performance in behavioral studies, and it is difficult to develop a task that is both sensitive enough and reliable enough to measure changes in the behavior of interest.

For instance, in the NO task, the methodology we used to interpret and score object recognition may not have accurately reflected exploratory behavior in mice. After scoring the number of entries into the exploratory zone of each object within a 5-minute span for each mouse at various time points, we noticed that the amount of time spent inside the exploratory zone during each entry were variable between mice, where some mice spent more time inside the exploratory zone while others spent less. Therefore, we thought that timing the total time each mouse spent at each object within the exploratory zone might give us different results. However, the results from this way of measuring exploration did not reflect what we found measuring the number of entries into the exploratory zone. In fact, it seemed that at a variety of time points, mice from different groups preferred to spend more time at the FO compared to the NO, which is contrary to normal mouse exploratory behavior.

One explanation for these unexpected results obtained by tracking the total amount of time spent at each object could be the way we defined exploratory behavior. We defined exploration as the time any part of the mouse, except for the tail, was within the exploratory zone, even when the mouse was facing away from the object or sitting on top of the object. Many researchers agree that climbing on the object by itself is not considered exploratory behavior (Leger et al., 2013). Some studies defined exploration as “directing the nose at a distance 2 cm or less to the object and/or touching it with the nose” (Antunes & Biala, 2012), which can be subjective, unless an operational definition was established for “directing the nose at the object”. In fact, some studies further define “directing the nose” as when the animal’s head is within 45 degrees of the object (Gaskin

et al., 2010; Mumby, Glenn, Nesbitt, & Kyriazis, 2002). In the future, we would like to adjust our operational definition of exploration to include a more specific and restrictive set of criteria than just when the animal is within 2 cm of the object, which might reduce variability and more accurately measure exploratory behavior. Another possibility is that there is no true difference in recognition memory between all four of the groups in our study.

We did not find any significant difference in performance at any of the time points in both the Y-maze task and the NO task between the HFD-fed animals and normal diet-fed animals that underwent sham surgery, suggesting that diet alone does not contribute to cognitive deficits. This is inconsistent with rodent studies showing that diet-induced obesity causes deficits in different cognitive processes including spatial memory and learning (Jurdak, Lichtenstein, & Kanarek, 2008; Nguyen, Killcross, & Jenkins, 2014). The discrepancies between our findings and those studies are most likely due to the differences in the composition of the diets, length of feeding period, and types of behavioral tasks used. For example, one study that found a memory deficit in obese animals used supplemental sugar to induce obesity in rats and used the Morris Water Maze to assess spatial memory and learning (Jurdak et al., 2008).

Although we were interested in the difference between the severity of cognitive deficits between the two diets at different time points after stroke, we were unable to observe any differences between these diet groups at 7 and 11 weeks. It is important to note that both the Y-maze and the NO task have a floor effect, meaning that the percent alternation or percent of NO contacts can only be lowered to a certain point. With this

issue of insensitivity at the lower end, any further cognitive deficits past a certain point will not be detected by these two behavioral tasks. Therefore, it is difficult to conclude from these behavioral tasks whether there was an actual difference in the severity of cognitive deficits between the two diet groups at 7 and 11 weeks after stroke. In the future, it may be useful to consider using more sensitive behavioral tasks.

Since we observed delayed-cognitive deficits in HFD-fed animals and normal diet-fed animals at different time points after stroke, we were interested in testing if these were associated with increased ischemic brain tissue atrophy. Using the three different methods of measuring brain tissue atrophy, we did not detect any difference in brain atrophy between HFD-fed animals and normal diet-fed animals 11 weeks after stroke. This is not altogether unexpected, since we did not see differences in cognitive deficits in HFD-fed and normal diet-fed animals at 11 weeks after stroke, the endpoint of the experiment at which we analyzed brain atrophy. Unfortunately, due to the limitations of our experimental design we were unable to analyze brain atrophy at the earlier time points, such as 4 and 7 weeks, when we did observe differences in cognitive deficit between the two diet groups. It is possible that the degree of brain atrophy is in fact greater at 1, 4, and 7 weeks after stroke in HFD-fed animals, associated with earlier onset of cognitive deficits. In the future, it may be useful to utilize a longitudinal measure of infarct size, such as MRI, over time during these different time points after stroke. This would allow us to analyze the relationship between the infarct size and cognitive performance from the same time points.

To characterize the neuroinflammatory response after stroke in the chronic phase in HFD-fed and normal diet-fed animals, we measured the extent of microgliosis/infiltration of monocyte-derived macrophages (MDMs) and astrogliosis in the peri-infarct area after stroke. Although a less inclusive and more inclusive threshold can qualitatively give us a percent area covered by cell bodies or reactive/activated cells, respectively, it is limited in that it cannot give us an exact cell count. Using less inclusive thresholding, we found that HFD-fed animals but not normal diet-fed animals have increased astrogliosis compared to the Control animals 11 weeks after stroke. However, both HFD-fed and normal diet-fed animals had increased astrogliosis at this time point using a more inclusive thresholding. The difference between our findings in the normal-diet group from using two thresholding techniques suggest that although the numbers of astrocytes in normal diet-fed animals are similar to the numbers found in Control animals at 11 weeks after stroke, the astrocytes in normal diet-animals adopt a more reactive phenotype compared to the astrocytes in Control animals at 11 weeks after stroke. On the other hand, our findings from the HFD-fed group suggest that there are significantly more astrocytes and that these adapt a more reactive phenotype compared to Control animals 11 weeks after stroke.

Our assessment of microgliosis found that normal diet-fed animals did not have increased microglia/MDM reactivity compared to Control animals 11 weeks after stroke. On the other hand, we demonstrated that HFD-fed animals had increased microgliosis compared to Control animals 11 weeks after stroke, regardless of the thresholding technique. These results suggest that HFD led to increased numbers of microglia/MDMs

that adapt a reactive phenotype at 11 weeks after stroke, and that the number of microglia/MDMs and their morphologies in normal diet-fed animals resemble what is seen before stroke.

Overall, we demonstrated that HFD animals persistently have more astrogliosis and microgliosis in the peri-infarct area even at such a late time point after stroke. It is possible that microglia and astrocytes that have migrated to the peri-infarct area and proliferated during the acute phase continued to reside there even during the chronic phase after stroke. On the other hand, we showed that the neuroinflammatory response in normal diet-fed animals may just be limited to astrogliosis at 11 weeks after stroke. Although studies show that astrocytes form a glial scar after stroke, which continues to remodel and persist in the chronic phase and beyond (Burda & Sofroniew, 2014), we were not able to assess if there were any differences in glial scarring between the two diet groups at 11 weeks after stroke since we only imaged the peri-infarct area for each animal. In the future, we would like to image the stroke border, which would allow us to assess glial scarring.

We did notice that three animals from the dMCAO-HFD group consistently had relatively darker CD68 and GFAP staining compared to the tissue sections seen in animals from the same group, and that this darker staining resulted in high levels of detected CD68 and GFAP coverage in the peri-infarct area in these three animals. We were unsure whether this relatively darker staining compared to those found in animals of the same group is a real biological difference and can be explained by biological variability, or if this difference is due to errors in processing of the tissue such as

ineffective perfusion of the brain or uneven immunostaining of the tissue sections. To resolve this issue, we plan to repeat the immunostaining to see if we can replicate these findings.

It is also worthy to discuss our finding that there were no differences in the GFAP and CD68 coverage using both inclusive and less inclusive thresholding between the HFD-fed animals that underwent sham and Control animals. This result suggests that diet alone cannot significantly change the degree of activation, proliferation, and/or migration of astrocytes and microglia. However, there is literature citing that diet-induced obesity leads to increased microglial proliferation in specific areas of the brain like the corpus callosum (Freeman, Haley-Zitlin, Stevens, & Granholm, 2011; Nguyen et al., 2014) and that astrogliosis can occur in other parts of the brain like the frontal cortex, parietal cortex, and hippocampus (Tomassoni et al., 2013). Again, the differences with our findings with the literature may be due to the differences in the methods of obesity induction and the areas in the brain that were analyzed. For example, the study by Freeman et al. (2011) found increased microgliosis in the hippocampus in diet-induced obese rats (Freeman et al., 2011), whereas we examined the cortex in a mouse model instead. This is consistent with recent findings in our laboratory, where we discovered minimal cortical gene changes between HFD and normal diet-fed animals prior to stroke, as measured by RNA sequencing (Peterson & Buckwalter, unpublished).

Lastly, we were interested in seeing whether the weight and diet of animals affected brain atrophy and the degree of neuroinflammation after stroke, which we measured by the amount of astrogliosis and microgliosis. Contrary to our original

hypothesis, we found that heavier animals did not necessarily have increased brain atrophy or increased astrogliosis compared to lighter animals. However, since we did not find significant differences in brain atrophy and astrogliosis between HFD-fed animals and normal diet-fed animals 11 weeks after stroke, it was not surprising that weight did not affect these two variables. On the other hand, we did find that the relationship between weight and the degree of microgliosis was significantly affected by diet condition. The HFD-fed animals that weighed more tended to also have more microgliosis compared to those HFD-fed animals that weighed less. However, this finding should be taken with caution. We noticed that the animals in the dMCAO-HFD group that had relatively darker CD68 staining compared to the animals in the same group happened to be the heavier ones in that group. Again, this result could be a true biological finding or could be due a coincidence where the darker staining due to ineffective tissue processing happened to occur with the tissues from heavier animals, therefore falsely driving the trend that we observed. This will be uncovered by future experiments.

In conclusion, we found an earlier onset of cognitive deficit in animals fed HFD compared to animals fed normal diet. Although we did not show that stroke size or brain atrophy was increased with HFD at 11 weeks after stroke, we did find more persistent neuroinflammation in HFD-fed mice at this time point. To further validate our results from the brain atrophy analysis, we also plan to measure the ipsilateral hemisphere area as a percent of the contralateral hemisphere area as well as the ipsilateral cortical area as a percent of the contralateral cortical area for both the Sham-normal diet and Sham-HFD

groups. This will provide us with a control, allowing us to know if the findings in the dMCAO-HFD group and the dMCAO-normal diet group were real biological findings, or if these findings were due to errors in our techniques, such as uneven sectioning of the brains. We also plan to image and threshold the stroke border for GFAP of all animals since we noticed more intense GFAP staining in those areas. Measuring the percent of stroke border covered by GFAP can possibly give us a more accurate reflection of the degree of glial scar formation. As mentioned earlier, we plan to troubleshoot our protocol for the NO task so that our measurements may more accurately reflect exploratory behavior in mice.

In the future, we would like to further examine the neuroinflammatory response in the chronic phase after ischemic stroke by looking at other immune cells including B-cells, T-cells, and dendritic cells, which are all shown to be a part of a larger adaptive inflammatory response that detrimentally affects cognitive functioning during the chronic phase (Doyle et al., 2015). Since Doyle et al.'s (2015) study also found T-cells and microglia/MDMs in certain areas of the thalamus, striatum, and internal capsule (Doyle et al., 2015), we would also like to see if we can also replicate these findings in our study to determine if the extent of adaptive and innate immune cell activity in these regions in the chronic phase after stroke differs between HFD-fed and normal diet-fed animals. Overall, we are interested in assessing whether the mechanisms of the responses of these other immune cells differ between HFD-fed animals and normal diet-fed animals and whether differences in immune responses correlate with and contribute to the cognitive deficits at the different time points we saw in this study.

## REFERENCES

- Abbas, A., Lichtman, A., & Pillai, S. (2016a). Antigen Capture and Presentation to Lymphocytes: what Lymphocytes See. In *Basic Immunology: Functions and Disorders of the Immune System* (5th ed.). St. Louis, Missouri: Elsevier.
- Abbas, A., Lichtman, A., & Pillai, S. (2016b). Effector Mechanisms of T Cell-Mediated Immunity: Functions of T Cells in Host Defense. In *Basic Immunology: Functions and Disorders of the Immune System* (5th ed.). St. Louis, Missouri: Elsevier.
- Abbas, A., Lichtman, A., & Pillai, S. (2016c). Humoral Immune Responses: Activation of B Lymphocytes and Production of Antibodies. In *Basic Immunology: Functions and Disorders of the Immune System* (5th ed.). St. Louis, Missouri: Elsevier.
- Abbas, A., Lichtman, A., & Pillai, S. (2016d). Innate Immunity: The Early Defense Against Infections. In *Basic Immunology: Functions and Disorders of the Immune System* (5th ed.). St. Louis, Missouri: Elsevier.
- Abbas, A., Lichtman, A., & Pillai, S. (2016e). Introduction to the Immune System: Nomenclature, General Properties, and Components. In *Basic Immunology: Functions and Disorders of the Immune System* (5th ed.). St. Louis, Missouri: Elsevier.

- Abbott, N. J. (2002). Astrocyte–endothelial interactions and blood–brain barrier permeability. *Journal of Anatomy*, *200*(6), 629–638.  
<https://doi.org/10.1046/j.1469-7580.2002.00064.x>
- Al-Qazzaz, N. K., Ali, S. H., Ahmad, S. A., Islam, S., & Mohamad, K. (2014). Cognitive impairment and memory dysfunction after a stroke diagnosis: a post-stroke memory assessment. *Neuropsychiatric Disease and Treatment*, *10*, 1677–1691.  
<https://doi.org/10.2147/NDT.S67184>
- Andersen, K. K., Olsen, T. S., Dehlendorff, C., & Kammergaard, L. P. (2009). Hemorrhagic and Ischemic Strokes Compared: Stroke Severity, Mortality, and Risk Factors. *Stroke*, *40*(6), 2068–2072.  
<https://doi.org/10.1161/STROKEAHA.108.540112>
- Antunes, M., & Biala, G. (2012). The novel object recognition memory: neurobiology, test procedure, and its modifications. *Cognitive Processing*, *13*(2), 93–110.  
<https://doi.org/10.1007/s10339-011-0430-z>
- Arumugam, T. V., Granger, D. N., & Mattson, M. P. (2005). Stroke and T-cells. *NeuroMolecular Medicine*, *7*(3), 229–242. <https://doi.org/10.1385/NMM:7:3:229>
- Asahi, M., Asahi, K., Jung, J.-C., Zoppo, G. J. del, Fini, M. E., & Lo, E. H. (2000). Role for Matrix Metalloproteinase 9 after Focal Cerebral Ischemia: Effects of Gene Knockout and Enzyme Inhibition with BB-94. *Journal of Cerebral Blood Flow & Metabolism*, *20*(12), 1681–1689. <https://doi.org/10.1097/00004647-200012000-00007>

- Benjamin, E. J., Blaha, M. J., Chiuve, S. E., Cushman, M., Das, S. R., Deo, R., ... Subcommittee, O. behalf of the A. H. A. S. C. and S. S. (2017). Heart Disease and Stroke Statistics—2017 Update: A Report From the American Heart Association. *Circulation*, CIR.0000000000000485.  
<https://doi.org/10.1161/CIR.0000000000000485>
- Benveniste, E. N. (1997). Cytokines: Influence on Glial Cell Gene Expression and Function. *Neuroimmunoendocrinology*, 69, 31–75.  
<https://doi.org/10.1159/000058653>
- Brait, V. H., Jackman, K. A., Walduck, A. K., Selemidis, S., Diep, H., Mast, A. E., ... Sobey, C. G. (2010). Mechanisms contributing to cerebral infarct size after stroke: gender, reperfusion, T lymphocytes, and Nox2-derived superoxide. *Journal of Cerebral Blood Flow and Metabolism: Official Journal of the International Society of Cerebral Blood Flow and Metabolism*, 30(7), 1306–1317.  
<https://doi.org/10.1038/jcbfm.2010.14>
- Bralet, A. M., Beley, A., Beley, P., & Bralet, J. (1979). Brain edema and blood-brain barrier permeability following quantitative cerebral microembolism. *Stroke*, 10(1), 34–38. <https://doi.org/10.1161/01.STR.10.1.34>
- Burda, J. E., & Sofroniew, M. V. (2014). Reactive gliosis and the multicellular response to CNS damage and disease. *Neuron*, 81(2), 229–248.  
<https://doi.org/10.1016/j.neuron.2013.12.034>
- Cao, X.-L., Du, J., Zhang, Y., Yan, J.-T., & Hu, X.-M. (2015). Hyperlipidemia exacerbates cerebral injury through oxidative stress, inflammation and neuronal

apoptosis in MCAO/reperfusion rats. *Experimental Brain Research*, 233(10), 2753–2765. <https://doi.org/10.1007/s00221-015-4269-x>

Caplan, L., Kasner, S., & Dashe, J. (2017, March 14). Etiology, classification, and epidemiology of stroke - UpToDate. Retrieved March 8, 2018, from [https://www.uptodate.com/contents/etiology-classification-and-epidemiology-of-stroke?search=stroke&source=search\\_result&selectedTitle=3~150&usage\\_type=default&display\\_rank=3#H7719405](https://www.uptodate.com/contents/etiology-classification-and-epidemiology-of-stroke?search=stroke&source=search_result&selectedTitle=3~150&usage_type=default&display_rank=3#H7719405)

Che, X., Ye, W., Panga, L., Wu, D.-C., & Yang, G.-Y. (2001). Monocyte chemoattractant protein-1 expressed in neurons and astrocytes during focal ischemia in mice. *Brain Research*, 902(2), 171–177. [https://doi.org/10.1016/S0006-8993\(01\)02328-9](https://doi.org/10.1016/S0006-8993(01)02328-9)

Chen, H., Song, Y. S., & Chan, P. H. (2009). Inhibition of NADPH Oxidase is Neuroprotective after Ischemia—Reperfusion. *Journal of Cerebral Blood Flow & Metabolism*, 29(7), 1262–1272. <https://doi.org/10.1038/jcbfm.2009.47>

Choudhury, G. R., & Ding, S. (2016). Reactive astrocytes and therapeutic potential in focal ischemic stroke. *Neurobiology of Disease*, 85, 234–244. <https://doi.org/10.1016/j.nbd.2015.05.003>

Chu, H. X., Kim, H. A., Lee, S., Moore, J. P., Chan, C. T., Vinh, A., ... Sobey, C. G. (2014). Immune cell infiltration in malignant middle cerebral artery infarction: comparison with transient cerebral ischemia. *Journal of Cerebral Blood Flow & Metabolism*, 34(3), 450–459. <https://doi.org/10.1038/jcbfm.2013.217>

- Claflin, E. S., Krishnan, C., & Khot, S. P. (2015). Emerging Treatments for Motor Rehabilitation After Stroke. *The Neurohospitalist*, *5*(2), 77–88.  
<https://doi.org/10.1177/1941874414561023>
- Conrad, C. D., Galea, L. A., Kuroda, Y., & McEwen, B. S. (1996). Chronic stress impairs rat spatial memory on the Y maze, and this effect is blocked by tianeptine pretreatment. *Behavioral Neuroscience*, *110*(6), 1321–1334.
- Davalos, D., Grutzendler, J., Yang, G., Kim, J. V., Zuo, Y., Jung, S., ... Gan, W.-B. (2005). ATP mediates rapid microglial response to local brain injury *in vivo*. *Nature Neuroscience*, *8*(6), 752–758. <https://doi.org/10.1038/nn1472>
- Deng, J., Zhang, J., Feng, C., Xiong, L., & Zuo, Z. (2014). Critical role of matrix metalloprotease-9 in chronic high fat diet-induced cerebral vascular remodelling and increase of ischaemic brain injury in mice. *Cardiovascular Research*, *103*(4), 473–484. <https://doi.org/10.1093/cvr/cvu154>
- Dhungana, H., Rolova, T., Savchenko, E., Wojciechowski, S., Savolainen, K., Ruotsalainen, A.-K., ... Malm, T. (2013). Western-type diet modulates inflammatory responses and impairs functional outcome following permanent middle cerebral artery occlusion in aged mice expressing the human apolipoprotein E4 allele. *Journal of Neuroinflammation*, *10*, 102.  
<https://doi.org/10.1186/1742-2094-10-102>
- Dong, Y., & Benveniste, E. N. (2001). Immune function of astrocytes. *Glia*, *36*(2), 180–190. <https://doi.org/10.1002/glia.1107>

- Doyle, K. P., & Buckwalter, M. S. (2014). A Mouse Model of Permanent Focal Ischemia: Distal Middle Cerebral Artery Occlusion. In *Cerebral Angiogenesis* (pp. 103–110). Humana Press, New York, NY. [https://doi.org/10.1007/978-1-4939-0320-7\\_9](https://doi.org/10.1007/978-1-4939-0320-7_9)
- Doyle, K. P., Fathali, N., Siddiqui, M. R., & Buckwalter, M. S. (2012). Distal hypoxic stroke: A new mouse model of stroke with high throughput, low variability and a quantifiable functional deficit. *Journal of Neuroscience Methods*, 207(1), 31–40. <https://doi.org/10.1016/j.jneumeth.2012.03.003>
- Doyle, K. P., Quach, L. N., Solé, M., Axtell, R. C., Nguyen, T.-V. V., Soler-Llavina, G. J., ... Buckwalter, M. S. (2015). B-Lymphocyte-Mediated Delayed Cognitive Impairment following Stroke. *Journal of Neuroscience*, 35(5), 2133–2145. <https://doi.org/10.1523/JNEUROSCI.4098-14.2015>
- Dvorianchikova, G., Barakat, D., Brambilla, R., Agudelo, C., Hernandez, E., Bethea, J. R., ... Ivanov, D. (2009). Inactivation of astroglial NF- $\kappa$ B promotes survival of retinal neurons following ischemic injury. *The European Journal of Neuroscience*, 30(2), 175–185. <https://doi.org/10.1111/j.1460-9568.2009.06814.x>
- Famakin, B. M. (2014). The Immune Response to Acute Focal Cerebral Ischemia and Associated Post-stroke Immunodepression: A Focused Review. *Aging and Disease*, 5(5), 307–326. <https://doi.org/10.14336/AD.2014.0500307>
- Farina, C., Aloisi, F., & Meinl, E. (2007). Astrocytes are active players in cerebral innate immunity. *Trends in Immunology*, 28(3), 138–145. <https://doi.org/10.1016/j.it.2007.01.005>

- Fawcett, J. W., & Asher, R. A. (1999). The glial scar and central nervous system repair. *Brain Research Bulletin*, 49(6), 377–391. [https://doi.org/10.1016/S0361-9230\(99\)00072-6](https://doi.org/10.1016/S0361-9230(99)00072-6)
- Feng, Y., Liao, S., Wei, C., Jia, D., Wood, K., Liu, Q., ... Jin, W.-N. (2017). Infiltration and persistence of lymphocytes during late-stage cerebral ischemia in middle cerebral artery occlusion and photothrombotic stroke models. *Journal of Neuroinflammation*, 14. <https://doi.org/10.1186/s12974-017-1017-0>
- Freeman, L. R., Haley-Zitlin, V., Stevens, C., & Granholm, A.-C. (2011). Diet-induced effects on neuronal and glial elements in the middle-aged rat hippocampus. *Nutritional Neuroscience*, 14(1), 32–44. <https://doi.org/10.1179/174313211X12966635733358>
- Fried, S. K., Bunkin, D. A., & Greenberg, A. S. (1998). Omental and Subcutaneous Adipose Tissues of Obese Subjects Release Interleukin-6: Depot Difference and Regulation by Glucocorticoid. *The Journal of Clinical Endocrinology & Metabolism*, 83(3), 847–850. <https://doi.org/10.1210/jcem.83.3.4660>
- Fruebis, J., Tsao, T.-S., Javorschi, S., Ebbets-Reed, D., Erickson, M. R. S., Yen, F. T., ... Lodish, H. F. (2001). Proteolytic cleavage product of 30-kDa adipocyte complement-related protein increases fatty acid oxidation in muscle and causes weight loss in mice. *Proceedings of the National Academy of Sciences of the United States of America*, 98(4), 2005–2010.
- Fu, Y., Chen, Y., Li, L., Wang, Y., Kong, X., & Wang, J. (2017). Food restriction affects Y-maze spatial recognition memory in developing mice. *International Journal of*

*Developmental Neuroscience*, 60, 8–15.

<https://doi.org/10.1016/j.ijdevneu.2017.03.010>

Garcia, J. H., Kalimo, H., Kamijyo, Y., & Trump, B. F. (1977). Cellular events during partial cerebral ischemia. I. Electron microscopy of feline cerebral cortex after middle-cerebral-artery occlusion. *Virchows Archiv. B, Cell Pathology*, 25(3), 191–206.

Gaskin, S., Tardif, M., Cole, E., Piterkin, P., Kayello, L., & Mumby, D. G. (2010). Object familiarization and novel-object preference in rats. *Behavioural Processes*, 83(1), 61–71. <https://doi.org/10.1016/j.beproc.2009.10.003>

Gelderblom, M., Leypoldt, F., Steinbach, K., Behrens, D., Choe, C.-U., Siler, D. A., ... Magnus, T. (2009). Temporal and Spatial Dynamics of Cerebral Immune Cell Accumulation in Stroke. *Stroke*, 40(5), 1849–1857. <https://doi.org/10.1161/STROKEAHA.108.534503>

Giraldo, E. (2017, February). Ischemic Stroke - Neurologic Disorders. Retrieved October 19, 2017, from <https://www.merckmanuals.com/professional/neurologic-disorders/stroke/ischemic-stroke>

Giulian, D., Corpuz, M., Chapman, S., Mansouri, M., & Robertson, C. (1993). Reactive mononuclear phagocytes release neurotoxins after ischemic and traumatic injury to the central nervous system. *Journal of Neuroscience Research*, 36(6), 681–693. <https://doi.org/10.1002/jnr.490360609>

- Greenberg, A. S., & Obin, M. S. (2006). Obesity and the role of adipose tissue in inflammation and metabolism. *The American Journal of Clinical Nutrition*, *83*(2), 461S-465S.
- Gregersen, R., Lambertsen, K., & Finsen, B. (2000). Microglia and Macrophages Are the Major Source of Tumor Necrosis Factor in Permanent Middle Cerebral Artery Occlusion in Mice. *Journal of Cerebral Blood Flow & Metabolism*, *20*(1), 53–65.  
<https://doi.org/10.1097/00004647-200001000-00009>
- Greter, M., Lelios, I., & Croxford, A. L. (2015). Microglia Versus Myeloid Cell Nomenclature during Brain Inflammation. *Frontiers in Immunology*, *6*.  
<https://doi.org/10.3389/fimmu.2015.00249>
- Grønberg, N. V., Johansen, F. F., Kristiansen, U., & Hasseldam, H. (2013). Leukocyte infiltration in experimental stroke. *Journal of Neuroinflammation*, *10*, 115.  
<https://doi.org/10.1186/1742-2094-10-115>
- Gu, L., Xiong, X., Zhang, H., Xu, B., Steinberg, G. K., & Zhao, H. (2012). Distinctive Effects of T Cell Subsets in Neuronal Injury Induced by Cocultured Splenocytes In Vitro and by In Vivo Stroke in Mice. *Stroke*, *43*(7), 1941–1946.  
<https://doi.org/10.1161/STROKEAHA.112.656611>
- Guo, Y., Yue, X., Li, H., Song, Z., Yan, H., Zhang, P., ... Li, T. (2016). Overweight and Obesity in Young Adulthood and the Risk of Stroke: a Meta-analysis. *Journal of Stroke and Cerebrovascular Diseases*, *25*(12), 2995–3004.  
<https://doi.org/10.1016/j.jstrokecerebrovasdis.2016.08.018>

- Halaas, J. L., Gajiwala, K. S., Maffei, M., Cohen, S. L., Chait, B. T., Rabinowitz, D., ... Friedman, J. M. (1995). Weight-reducing effects of the plasma protein encoded by the obese gene. *Science*, *269*(5223), 543–546.  
<https://doi.org/10.1126/science.7624777>
- Haley, M. J., Krishnan, S., Burrows, D., Hoog, L. de, Thakrar, J., Schiessl, I., ... Lawrence, C. B. (2017). Acute high-fat feeding leads to disruptions in glucose homeostasis and worsens stroke outcome. *Journal of Cerebral Blood Flow & Metabolism*, *0271678X17744718*. <https://doi.org/10.1177/0271678X17744718>
- Haley, M. J., & Lawrence, C. B. (2016). Obesity and stroke: Can we translate from rodents to patients? *Journal of Cerebral Blood Flow and Metabolism: Official Journal of the International Society of Cerebral Blood Flow and Metabolism*, *36*(12), 2007–2021. <https://doi.org/10.1177/0271678X16670411>
- Hallenbeck, J. M., Dutka, A. J., Tanishima, T., Kochanek, P. M., Kumaroo, K. K., Thompson, C. B., ... Contreras, T. J. (1986). Polymorphonuclear leukocyte accumulation in brain regions with low blood flow during the early postischemic period. *Stroke*, *17*(2), 246–253. <https://doi.org/10.1161/01.STR.17.2.246>
- Hayakawa, K., Nakano, T., Irie, K., Higuchi, S., Fujioka, M., Orito, K., ... Fujiwara, M. (2010). Inhibition of Reactive Astrocytes with Fluorocitrate Retards Neurovascular Remodeling and Recovery after Focal Cerebral Ischemia in Mice. *Journal of Cerebral Blood Flow & Metabolism*, *30*(4), 871–882.  
<https://doi.org/10.1038/jcbfm.2009.257>

- Hotamisligil, G. S., Shargill, N. S., & Spiegelman, B. M. (1993). Adipose expression of tumor necrosis factor- $\alpha$ : direct role in obesity-linked insulin resistance. *Science*, *259*(5091), 87–91. <https://doi.org/10.1126/science.7678183>
- Hu, X., Leak, R. K., Shi, Y., Suenaga, J., Gao, Y., Zheng, P., & Chen, J. (2015). Microglial and macrophage polarization-new prospects for brain repair. *Nature Reviews. Neurology*, *11*(1), 56–64. <https://doi.org/10.1038/nrneurol.2014.207>
- Hu, X., Li, P., Guo, Y., Wang, H., Leak, R. K., Chen, S., ... Chen, J. (2012). Microglia/macrophage polarization dynamics reveal novel mechanism of injury expansion after focal cerebral ischemia. *Stroke*, *43*(11), 3063–3070. <https://doi.org/10.1161/STROKEAHA.112.659656>
- Huang, J., Upadhyay, U. M., & Tamargo, R. J. (2006). Inflammation in stroke and focal cerebral ischemia. *Surgical Neurology*, *66*(3), 232–245. <https://doi.org/10.1016/j.surneu.2005.12.028>
- Huh, J. Y., Park, Y. J., Ham, M., & Kim, J. B. (2014). Crosstalk between Adipocytes and Immune Cells in Adipose Tissue Inflammation and Metabolic Dysregulation in Obesity. *Molecules and Cells*, *37*(5), 365–371. <https://doi.org/10.14348/molcells.2014.0074>
- Imai, F., Suzuki, H., Oda, J., Ninomiya, T., Ono, K., Sano, H., & Sawada, M. (2007). Neuroprotective Effect of Exogenous Microglia in Global Brain Ischemia. *Journal of Cerebral Blood Flow & Metabolism*, *27*(3), 488–500. <https://doi.org/10.1038/sj.jcbfm.9600362>

- Inose, Y., Kato, Y., Kitagawa, K., Uchiyama, S., & Shibata, N. (2015). Activated microglia in ischemic stroke penumbra upregulate MCP-1 and CCR2 expression in response to lysophosphatidylcholine derived from adjacent neurons and astrocytes. *Neuropathology*, 35(3), 209–223. <https://doi.org/10.1111/neup.12182>
- Jander, S., Kraemer, M., Schroeter, M., Witte, O. W., & Stoll, G. (1995). Lymphocytic Infiltration and Expression of Intercellular Adhesion Molecule-1 in Photochemically Induced Ischemia of the Rat Cortex. *Journal of Cerebral Blood Flow & Metabolism*, 15(1), 42–51. <https://doi.org/10.1038/jcbfm.1995.5>
- Jickling, G. C., Liu, D., Ander, B. P., Stamova, B., Zhan, X., & Sharp, F. R. (2015). Targeting neutrophils in ischemic stroke: translational insights from experimental studies. *Journal of Cerebral Blood Flow & Metabolism*, 35(6), 888–901. <https://doi.org/10.1038/jcbfm.2015.45>
- Jurdak, N., Lichtenstein, A. H., & Kanarek, R. B. (2008). Diet-induced obesity and spatial cognition in young male rats. *Nutritional Neuroscience*, 11(2), 48–54. <https://doi.org/10.1179/147683008X301333>
- Justicia, C., Panés, J., Solé, S., Cervera, Á., Deulofeu, R., Chamorro, Á., & Planas, A. M. (2003). Neutrophil Infiltration Increases Matrix Metalloproteinase-9 in the Ischemic Brain after Occlusion/Reperfusion of the Middle Cerebral Artery in Rats. *Journal of Cerebral Blood Flow & Metabolism*, 23(12), 1430–1440. <https://doi.org/10.1097/01.WCB.0000090680.07515.C8>
- Kanda, H., Tateya, S., Tamori, Y., Kotani, K., Hiasa, K., Kitazawa, R., ... Kasuga, M. (2006). MCP-1 contributes to macrophage infiltration into adipose tissue, insulin

- resistance, and hepatic steatosis in obesity. *Journal of Clinical Investigation*, 116(6), 1494–1505. <https://doi.org/10.1172/JCI26498>
- Kang, K., Reilly, S. M., Karabacak, V., Gangl, M. R., Fitzgerald, K., Hatano, B., & Lee, C.-H. (2008). Adipocyte-Derived Th2 Cytokines and Myeloid PPAR $\delta$  Regulate Macrophage Polarization and Insulin Sensitivity. *Cell Metabolism*, 7(6), 485–495. <https://doi.org/10.1016/j.cmet.2008.04.002>
- Karikó, K., Ni, H., Capodici, J., Lamphier, M., & Weissman, D. (2004). mRNA Is an Endogenous Ligand for Toll-like Receptor 3. *Journal of Biological Chemistry*, 279(13), 12542–12550. <https://doi.org/10.1074/jbc.M310175200>
- Karikó, K., Weissman, D., & Welsh, F. A. (2004). Inhibition of Toll-like Receptor and Cytokine Signaling—A Unifying Theme in Ischemic Tolerance. *Journal of Cerebral Blood Flow & Metabolism*, 24(11), 1288–1304. <https://doi.org/10.1097/01.WCB.0000145666.68576.71>
- Kawabori, M., & Yenari, M. A. (2015). The role of the microglia in acute CNS injury. *Metabolic Brain Disease*, 30(2), 381–392. <https://doi.org/10.1007/s11011-014-9531-6>
- Kim, E., Tolhurst, A. T., & Cho, S. (2014). Deregulation of inflammatory response in the diabetic condition is associated with increased ischemic brain injury. *Journal of Neuroinflammation*, 11(1), 83. <https://doi.org/10.1186/1742-2094-11-83>
- Kim, J. Y., Park, J., Chang, J. Y., Kim, S.-H., & Lee, J. E. (2016). Inflammation after Ischemic Stroke: The Role of Leukocytes and Glial Cells. *Experimental Neurobiology*, 25(5), 241–251. <https://doi.org/10.5607/en.2016.25.5.241>

- Kleinschnitz, C., Schwab, N., Kraft, P., Hagedorn, I., Dreykluft, A., Schwarz, T., ...  
Stoll, G. (2010). Early detrimental T-cell effects in experimental cerebral  
ischemia are neither related to adaptive immunity nor thrombus formation. *Blood*,  
*115*(18), 3835–3842. <https://doi.org/10.1182/blood-2009-10-249078>
- Kumari, R., Willing, L. B., Patel, S. D., Baskerville, K. A., & Simpson, I. A. (2011).  
Increased Cerebral Matrix Metalloprotease -9 Activity is Associated with  
Compromised Recovery in the Diabetic db/db Mouse Following a Stroke. *Journal  
of Neurochemistry*, *119*(5), 1029–1040. <https://doi.org/10.1111/j.1471-4159.2011.07487.x>
- Lawrence, E. S., Coshall, C., Dundas, R., Stewart, J., Rudd, A. G., Howard, R., & Wolfe,  
C. D. A. (2001). Estimates of the Prevalence of Acute Stroke Impairments and  
Disability in a Multiethnic Population. *Stroke*, *32*(6), 1279–1284.  
<https://doi.org/10.1161/01.STR.32.6.1279>
- Lee, G. H., Proenca, R., Montez, J. M., Carroll, K. M., Darvishzadeh, J. G., Lee, J. I., &  
Friedman, J. M. (1996). Abnormal splicing of the leptin receptor in diabetic mice.  
*Nature*, *379*(6566), 632–635. <https://doi.org/10.1038/379632a0>
- Leger, M., Quiedeville, A., Bouet, V., Haelewyn, B., Boulouard, M., Schumann-Bard, P.,  
& Freret, T. (2013). Object recognition test in mice. *Nature Protocols*, *8*(12),  
2531–2537. <https://doi.org/10.1038/nprot.2013.155>
- Li, P., Quan, W., Lu, D., Wang, Y., Zhang, H.-H., Liu, S., ... Zhou, Y.-Y. (2016).  
Association between Metabolic Syndrome and Cognitive Impairment after Acute

- Ischemic Stroke: A Cross-Sectional Study in a Chinese Population. *PLoS ONE*, 11(12), e0167327. <https://doi.org/10.1371/journal.pone.0167327>
- Li, T., Pang, S., Yu, Y., Wu, X., Guo, J., & Zhang, S. (2013). Proliferation of parenchymal microglia is the main source of microgliosis after ischaemic stroke. *Brain*, 136(12), 3578–3588. <https://doi.org/10.1093/brain/awt287>
- Li, T., & Zhang, S. (2016). Microgliosis in the Injured Brain: Infiltrating Cells and Reactive Microglia Both Play a Role. *The Neuroscientist*, 22(2), 165–170. <https://doi.org/10.1177/1073858415572079>
- Liddelow, S. A., Guttenplan, K. A., Clarke, L. E., Bennett, F. C., Bohlen, C. J., Schirmer, L., ... Barres, B. A. (2017). Neurotoxic reactive astrocytes are induced by activated microglia. *Nature*, 541(7638), 481–487. <https://doi.org/10.1038/nature21029>
- Lu, D., Ren, S., Zhang, J., & Sun, D. (2016). Vascular risk factors aggravate cognitive impairment in first-ever young ischaemic stroke patients. *European Journal of Neurology*, 23(5), 940–947. <https://doi.org/10.1111/ene.12967>
- Lumeng, C. N., Bodzin, J. L., & Saltiel, A. R. (2007). Obesity induces a phenotypic switch in adipose tissue macrophage polarization. *Journal of Clinical Investigation*, 117(1), 175–184. <https://doi.org/10.1172/JCI29881>
- Maysami, S., Haley, M. J., Gorenkova, N., Krishnan, S., McColl, B. W., & Lawrence, C. B. (2015). Prolonged diet-induced obesity in mice modifies the inflammatory response and leads to worse outcome after stroke. *Journal of Neuroinflammation*, 12, 140. <https://doi.org/10.1186/s12974-015-0359-8>

- Meschia, J. F., Bushnell, C., Boden-Albala, B., Braun, L. T., Bravata, D. M., Chaturvedi, S., ... Wilson, J. A. (2014). Guidelines for the Primary Prevention of Stroke. *Stroke; a Journal of Cerebral Circulation*, 45(12), 3754–3832.  
<https://doi.org/10.1161/STR.0000000000000046>
- Mitchell, A. B., Cole, J. W., McArdle, P. F., Cheng, Y.-C., Ryan, K. A., Sparks, M. J., ... Kittner, S. J. (2015). Obesity Increases Risk of Ischemic Stroke in Young Adults. *Stroke*, STROKEAHA.115.008940.  
<https://doi.org/10.1161/STROKEAHA.115.008940>
- Molofsky, A. B., Nussbaum, J. C., Liang, H.-E., Van Dyken, S. J., Cheng, L. E., Mohapatra, A., ... Locksley, R. M. (2013). Innate lymphoid type 2 cells sustain visceral adipose tissue eosinophils and alternatively activated macrophages. *The Journal of Experimental Medicine*, 210(3), 535–549.  
<https://doi.org/10.1084/jem.20121964>
- Muldoon, L. L., Alvarez, J. I., Begley, D. J., Boado, R. J., del Zoppo, G. J., Doolittle, N. D., ... Neuwelt, E. A. (2013). Immunologic privilege in the central nervous system and the blood–brain barrier. *Journal of Cerebral Blood Flow & Metabolism*, 33(1), 13–21. <https://doi.org/10.1038/jcbfm.2012.153>
- Mumby, D. G., Glenn, M. J., Nesbitt, C., & Kyriazis, D. A. (2002). Dissociation in retrograde memory for object discriminations and object recognition in rats with perirhinal cortex damage. *Behavioural Brain Research*, 132(2), 215–226.  
[https://doi.org/10.1016/S0166-4328\(01\)00444-2](https://doi.org/10.1016/S0166-4328(01)00444-2)

- Nature Neuroscience. (2009). Troublesome variability in mouse studies. *Nature Neuroscience*, *12*(9), 1075. <https://doi.org/10.1038/nn0909-1075>
- Nawashiro, H., Brenner, M., Fukui, S., Shima, K., & Hallenbeck, J. M. (2000). High Susceptibility to Cerebral Ischemia in GFAP-Null Mice. *Journal of Cerebral Blood Flow & Metabolism*, *20*(7), 1040–1044. <https://doi.org/10.1097/00004647-200007000-00003>
- Neumann, J., Gunzer, M., Gutzeit, H. O., Ullrich, O., Reymann, K. G., & Dinkel, K. (2006). Microglia provide neuroprotection after ischemia. *The FASEB Journal*, *20*(6), 714–716. <https://doi.org/10.1096/fj.05-4882fje>
- Nguyen, J. C. D., Killcross, A. S., & Jenkins, T. A. (2014). Obesity and cognitive decline: role of inflammation and vascular changes. *Frontiers in Neuroscience*, *8*. <https://doi.org/10.3389/fnins.2014.00375>
- Nilsson, L.-G., & Nilsson, E. (2009). Overweight and cognition. *Scandinavian Journal of Psychology*, *50*(6), 660–667. <https://doi.org/10.1111/j.1467-9450.2009.00777.x>
- Nimmerjahn, A., Kirchhoff, F., & Helmchen, F. (2005). Resting Microglial Cells Are Highly Dynamic Surveillants of Brain Parenchyma in Vivo. *Science*, *308*(5726), 1314–1318. <https://doi.org/10.1126/science.1110647>
- Nishimura, S., Manabe, I., Nagasaki, M., Eto, K., Yamashita, H., Ohsugi, M., ... Nagai, R. (2009). CD8+ effector T cells contribute to macrophage recruitment and adipose tissue inflammation in obesity. *Nature Medicine*, *15*(8), 914–920. <https://doi.org/10.1038/nm.1964>

- Nishimura, S., Manabe, I., Takaki, S., Nagasaki, M., Otsu, M., Yamashita, H., ... Nagai, R. (2013). Adipose Natural Regulatory B Cells Negatively Control Adipose Tissue Inflammation. *Cell Metabolism*, 18(5), 759–766.  
<https://doi.org/10.1016/j.cmet.2013.09.017>
- Okamura, Y., Watari, M., Jerud, E. S., Young, D. W., Ishizaka, S. T., Rose, J., ... Strauss, J. F. (2001). The Extra Domain A of Fibronectin Activates Toll-like Receptor 4. *Journal of Biological Chemistry*, 276(13), 10229–10233.  
<https://doi.org/10.1074/jbc.M100099200>
- Olson, J. K., & Miller, S. D. (2004). Microglia Initiate Central Nervous System Innate and Adaptive Immune Responses through Multiple TLRs. *The Journal of Immunology*, 173(6), 3916–3924. <https://doi.org/10.4049/jimmunol.173.6.3916>
- Panickar, K. S., & Norenberg, M. D. (2005). Astrocytes in cerebral ischemic injury: Morphological and general considerations. *Glia*, 50(4), 287–298.  
<https://doi.org/10.1002/glia.20181>
- Patel, A. R., Ritzel, R., McCullough, L. D., & Liu, F. (2013). Microglia and ischemic stroke: a double-edged sword. *International Journal of Physiology, Pathophysiology and Pharmacology*, 5(2), 73–90.
- Peterson, T., & Buckwalter, M. (n.d.). *Minimal cortical gene differences between obese mice and mice with normal weight*. unpublished.
- Reisel, D., Bannerman, D. M., Schmitt, W. B., Deacon, R. M. J., Flint, J., Borchardt, T., ... Rawlins, J. N. P. (2002). Spatial memory dissociations in mice lacking GluR1. *Nature Neuroscience*, 5(9), 868–873. <https://doi.org/10.1038/nn910>

- Ren, X., Akiyoshi, K., Dziennis, S., Vandenbark, A. A., Herson, P. S., Hurn, P. D., & Offner, H. (2011). Regulatory B Cells Limit CNS Inflammation and Neurologic Deficits in Murine Experimental Stroke. *Journal of Neuroscience*, *31*(23), 8556–8563. <https://doi.org/10.1523/JNEUROSCI.1623-11.2011>
- Rosenberg, G. A., Estrada, E. Y., & Dencoff, J. E. (1998). Matrix Metalloproteinases and TIMPs Are Associated With Blood-Brain Barrier Opening After Reperfusion in Rat Brain. *Stroke*, *29*(10), 2189–2195. <https://doi.org/10.1161/01.STR.29.10.2189>
- Sartipy, P., & Loskutoff, D. J. (2003). Monocyte chemoattractant protein 1 in obesity and insulin resistance. *Proceedings of the National Academy of Sciences of the United States of America*, *100*(12), 7265–7270. <https://doi.org/10.1073/pnas.1133870100>
- Schroeter, M., Jander, S., Witte, O. W., & Stoll, G. (1994). Local immune responses in the rat cerebral cortex after middle cerebral artery occlusion. *Journal of Neuroimmunology*, *55*(2), 195–203. [https://doi.org/10.1016/0165-5728\(94\)90010-8](https://doi.org/10.1016/0165-5728(94)90010-8)
- Schuhmann, M. K., Langhauser, F., Kraft, P., & Kleinschnitz, C. (2017). B cells do not have a major pathophysiologic role in acute ischemic stroke in mice. *Journal of Neuroinflammation*, *14*. <https://doi.org/10.1186/s12974-017-0890-x>
- Shi, H., Kokoeva, M. V., Inouye, K., Tzameli, I., Yin, H., & Flier, J. S. (2006). TLR4 links innate immunity and fatty acid–induced insulin resistance. *Journal of Clinical Investigation*, *116*(11), 3015–3025. <https://doi.org/10.1172/JCI28898>

- Slater, D. (2018). Middle Cerebral Artery Stroke: Overview, Rehabilitation Setting Selection and Indications, Best Practices. Retrieved from <https://emedicine.medscape.com/article/323120-overview>
- Sousa N., Almeida O. F. X., & Wotjak C. T. (2006). A hitchhiker's guide to behavioral analysis in laboratory rodents. *Genes, Brain and Behavior*, 5(s2), 5–24. <https://doi.org/10.1111/j.1601-183X.2006.00228.x>
- Stanford Medicine. (2017). Y Maze Spontaneous Alternation Test | Behavioral and Functional Neuroscience Laboratory | Stanford Medicine. Retrieved March 15, 2018, from <http://med.stanford.edu/sbfnl/services/bm/lm/y-maze.html>
- Stanimirovic, D. B., Wong, J., Shapiro, A., & Durkin, J. P. (1997). Increase in surface expression of ICAM-1, VCAM-1 and E-selectin in human cerebrovascular endothelial cells subjected to ischemia-like insults. *Acta Neurochirurgica. Supplement*, 70, 12–16.
- Stevens, S. L., Bao, J., Hollis, J., Lessov, N. S., Clark, W. M., & Stenzel-Poore, M. P. (2002). The use of flow cytometry to evaluate temporal changes in inflammatory cells following focal cerebral ischemia in mice. *Brain Research*, 932(1), 110–119. [https://doi.org/10.1016/S0006-8993\(02\)02292-8](https://doi.org/10.1016/S0006-8993(02)02292-8)
- Stienstra, R., Diepen, J. A. van, Tack, C. J., Zaki, M. H., Veerdonk, F. L. van de, Perera, D., ... Kanneganti, T.-D. (2011). Inflammasome is a central player in the induction of obesity and insulin resistance. *Proceedings of the National Academy of Sciences*, 108(37), 15324–15329. <https://doi.org/10.1073/pnas.1100255108>

- Stienstra, R., Joosten, L. A. B., Koenen, T., Tits, B. van, Diepen, J. A. van, Berg, S. A. A. van den, ... Netea, M. G. (2010). The Inflammasome-Mediated Caspase-1 Activation Controls Adipocyte Differentiation and Insulin Sensitivity. *Cell Metabolism*, 12(6), 593–605. <https://doi.org/10.1016/j.cmet.2010.11.011>
- Stockinger, B., Veldhoen, M., & Martin, B. (2007). Th17 T cells: Linking innate and adaptive immunity. *Seminars in Immunology*, 19(6), 353–361. <https://doi.org/10.1016/j.smim.2007.10.008>
- Strazzullo, P., D'Elia, L., Cairella, G., Garbagnati, F., Cappuccio, F. P., & Scalfi, L. (2010). Excess Body Weight and Incidence of Stroke: Meta-Analysis of Prospective Studies With 2 Million Participants. *Stroke*, 41(5), e418–e426. <https://doi.org/10.1161/STROKEAHA.109.576967>
- Suk, S.-H., Sacco, R. L., Boden-Albala, B., Cheun, J. F., Pittman, J. G., Elkind, M. S., & Paik, M. C. (2003). Abdominal Obesity and Risk of Ischemic Stroke: The Northern Manhattan Stroke Study. *Stroke*, 34(7), 1586–1592. <https://doi.org/10.1161/01.STR.0000075294.98582.2F>
- Sun, J.-H., Tan, L., & Yu, J.-T. (2014). Post-stroke cognitive impairment: epidemiology, mechanisms and management. *Annals of Translational Medicine*, 2(8). <https://doi.org/10.3978/j.issn.2305-5839.2014.08.05>
- Takano, T., Oberheim, N., Cotrina, M. L., & Nedergaard, M. (2009). Astrocytes and ischemic injury. *Stroke; a Journal of Cerebral Circulation*, 40(3 Suppl), S8-12. <https://doi.org/10.1161/STROKEAHA.108.533166>

- Tamura, A., Graham, D. I., McCulloch, J., & Teasdale, G. M. (1981). Focal Cerebral Ischaemia in the Rat: 1. Description of Technique and Early Neuropathological Consequences following Middle Cerebral Artery Occlusion. *Journal of Cerebral Blood Flow & Metabolism*, *1*(1), 53–60. <https://doi.org/10.1038/jcbfm.1981.6>
- Terao, S., Yilmaz, G., Stokes, K. Y., Ishikawa, M., Kawase, T., & Granger, D. N. (2008). Inflammatory and Injury Responses to Ischemic Stroke in Obese Mice. *Stroke*, *39*(3), 943–950. <https://doi.org/10.1161/STROKEAHA.107.494542>
- The Jackson Laboratory. (2018). Body Weight Information for C57BL/6J (000664). Retrieved March 22, 2018, from <https://www.jax.org/jax-mice-and-services/strain-data-sheet-pages/body-weight-chart-000664>
- Tiemessen, M. M., Jagger, A. L., Evans, H. G., Herwijnen, M. J. C. van, John, S., & Taams, L. S. (2007). CD4+CD25+Foxp3+ regulatory T cells induce alternative activation of human monocytes/macrophages. *Proceedings of the National Academy of Sciences of the United States of America*, *104*(49), 19446–19451. <https://doi.org/10.1073/pnas.0706832104>
- Tomassoni, D., Nwankwo, I. E., Gabrielli, M. G., Bhatt, S., Muhammad, A. B., Lokhandwala, M. F., ... Amenta, F. (2013). Astrogliosis in the brain of obese Zucker rat: A model of metabolic syndrome. *Neuroscience Letters*, *543*, 136–141. <https://doi.org/10.1016/j.neulet.2013.03.025>
- Trayhurn, P., & Wood, I. S. (2004). Adipokines: inflammation and the pleiotropic role of white adipose tissue. *British Journal of Nutrition*, *92*(3), 347–355. <https://doi.org/10.1079/BJN20041213>

- Turner, R. J., & Sharp, F. R. (2016). Implications of MMP9 for Blood Brain Barrier Disruption and Hemorrhagic Transformation Following Ischemic Stroke. *Frontiers in Cellular Neuroscience, 10*. <https://doi.org/10.3389/fncel.2016.00056>
- U.S Department of Health and Human Services. (2018, August). Overweight & Obesity Statistics | NIDDK. Retrieved February 11, 2018, from <https://www.niddk.nih.gov/health-information/health-statistics/overweight-obesity>
- Vandanmagsar, B., Youm, Y.-H., Ravussin, A., Galgani, J. E., Stadler, K., Mynatt, R. L., ... Dixit, V. D. (2011). The NLRP3 inflammasome instigates obesity-induced inflammation and insulin resistance. *Nature Medicine, 17*(2), 179–188. <https://doi.org/10.1038/nm.2279>
- Vindegard, N., Muñoz-Briones, C., El Ali, H. H., Kristensen, L. K., Rasmussen, R. S., Johansen, F. F., & Hasseldam, H. (2017). T-cells and macrophages peak weeks after experimental stroke: Spatial and temporal characteristics. *Neuropathology, 37*(5), 407–414. <https://doi.org/10.1111/neup.12387>
- Wang, R.-X., Yu, C.-R., Dambuza, I. M., Mahdi, R. M., Dolinska, M. B., Sergeev, Y. V., ... Egwuagu, C. E. (2014). Interleukin-35 induces regulatory B cells that suppress autoimmune disease. *Nature Medicine, 20*(6), 633–641. <https://doi.org/10.1038/nm.3554>
- Wang, W., Redecker, C., Yu, Z.-Y., Xie, M.-J., Tian, D.-S., Zhang, L., ... Witte, O. W. (2008). Rat focal cerebral ischemia induced astrocyte proliferation and delayed neuronal death are attenuated by cyclin-dependent kinase inhibition. *Journal of*

*Clinical Neuroscience: Official Journal of the Neurosurgical Society of Australasia*, 15(3), 278–285. <https://doi.org/10.1016/j.jocn.2007.02.004>

Weisberg, S. P., McCann, D., Desai, M., Rosenbaum, M., Leibel, R. L., & Ferrante, A. W. (2003). Obesity is associated with macrophage accumulation in adipose tissue. *The Journal of Clinical Investigation*, 112(12), 1796–1808. <https://doi.org/10.1172/JCI19246>

Winer, D. A., Winer, S., Shen, L., Wadia, P. P., Yantha, J., Paltser, G., ... Engleman, E. G. (2011). B cells promote insulin resistance through modulation of T cells and production of pathogenic IgG antibodies. *Nature Medicine*, 17(5), 610–617. <https://doi.org/10.1038/nm.2353>

Winer, S., Chan, Y., Paltser, G., Truong, D., Tsui, H., Bahrami, J., ... Dosch, H.-M. (2009). Normalization of obesity-associated insulin resistance through immunotherapy. *Nature Medicine*, 15(8), 921–929. <https://doi.org/10.1038/nm.2001>

World Health Organization. (2018a). WHO | Obesity. Retrieved February 11, 2018, from [http://www.who.int/gho/ncd/risk\\_factors/obesity\\_text/en/](http://www.who.int/gho/ncd/risk_factors/obesity_text/en/)

World Health Organization. (2018b, February). WHO | Obesity and overweight. Retrieved February 11, 2018, from <http://www.who.int/mediacentre/factsheets/fs311/en/>

Wu, D., Molofsky, A. B., Liang, H.-E., Ricardo-Gonzalez, R. R., Jouihan, H. A., Bando, J. K., ... Locksley, R. M. (2011). Eosinophils sustain adipose alternatively

- activated macrophages associated with glucose homeostasis. *Science (New York, N.Y.)*, 332(6026), 243–247. <https://doi.org/10.1126/science.1201475>
- Wykes, M., & Macpherson, G. (2000). Dendritic cell–B-cell interaction: dendritic cells provide B cells with CD40-independent proliferation signals and CD40-dependent survival signals. *Immunology*, 100(1), 1–3. <https://doi.org/10.1046/j.1365-2567.2000.00044.x>
- Yamauchi, T., Kamon, J., Waki, H., Terauchi, Y., Kubota, N., Hara, K., ... Kadowaki, T. (2001). The fat-derived hormone adiponectin reverses insulin resistance associated with both lipodystrophy and obesity. *Nature Medicine*, 7(8), 941–946. <https://doi.org/10.1038/90984>
- Yang, Q. (2017). Vital Signs: Recent Trends in Stroke Death Rates — United States, 2000–2015. *MMWR. Morbidity and Mortality Weekly Report*, 66. <https://doi.org/10.15585/mmwr.mm6635e1>
- Zhang, R., Chopp, M., Zhang, Z., Jiang, N., & Powers, C. (1998). The expression of P- and E-selectins in three models of middle cerebral artery occlusion. *Brain Research*, 785(2), 207–214. [https://doi.org/10.1016/S0006-8993\(97\)01343-7](https://doi.org/10.1016/S0006-8993(97)01343-7)
- Zhang, T., Pan, B.-S., Zhao, B., Zhang, L.-M., Huang, Y.-L., & Sun, F.-Y. (2009). Exacerbation of poststroke dementia by type 2 diabetes is associated with synergistic increases of  $\beta$ -secretase activation and  $\beta$ -amyloid generation in rat brains. *Neuroscience*, 161(4), 1045–1056. <https://doi.org/10.1016/j.neuroscience.2009.04.032>

- Zhang, Ting, Pan, B.-S., Sun, G.-C., Sun, X., & Sun, F.-Y. (2010). Diabetes synergistically exacerbates poststroke dementia and tau abnormality in brain. *Neurochemistry International*, *56*(8), 955–961.  
<https://doi.org/10.1016/j.neuint.2010.04.003>
- Zhang, Y., Proenca, R., Maffei, M., Barone, M., Leopold, L., & Friedman, J. M. (1994). Positional cloning of the mouse obese gene and its human homologue. *Nature*, *372*(6505), 425–432. <https://doi.org/10.1038/372425a0>
- Zhang, Yong, Zhang, Z., Yang, B., Li, Y., Zhang, Q., Qu, Q., ... Xu, T. (2012). Incidence and risk factors of cognitive impairment 3 months after first-ever stroke: A cross-sectional study of 5 geographic areas of China. *Journal of Huazhong University of Science and Technology [Medical Sciences]*, *32*(6), 906–911.  
<https://doi.org/10.1007/s11596-012-1056-9>
- Zhang, Z. G., & Chopp, M. (2015). Promoting brain remodeling to aid in stroke recovery. *Trends in Molecular Medicine*, *21*(9), 543–548.  
<https://doi.org/10.1016/j.molmed.2015.07.005>
- Zhao, H., Wan, L., Chen, Y., Zhang, H., Xu, Y., & Qiu, S. (2018). FasL incapacitation alleviates CD4<sup>+</sup> T cells-induced brain injury through remodeling of microglia polarization in mouse ischemic stroke. *Journal of Neuroimmunology*.  
<https://doi.org/10.1016/j.jneuroim.2018.01.017>

**CURRICULUM VITAE**

